



**JIMMA UNIVERSITY**  
**SCHOOL OF GRADUATE STUDIES**  
**JIMMA INSTITUTE OF TECHNOLOGY**  
**FACULTY OF CIVIL AND ENVIRONMENTAL ENGINEERING**  
**HYDROLOGY AND HYDRAULIC ENGINEERING CHAIR**

**Watershed Hydrological Responses to Changes in Land Use and Land Cover at Hangar Watershed, Ethiopia.**

By  
Abdata Wakjira Galata

A Thesis Submitted to School of Graduate Studies of Jimma University in Partial Fulfillment of the Requirements for the Degree of Master of Science in Hydraulic Engineering.

January, 2019  
Jimma, Ethiopia

**JIMMA UNIVERSITY**  
**SCHOOL OF GRADUATE STUDIES**  
**JIMMA INSTITUTE OF TECHNOLOGY**  
**FACULTY OF CIVIL AND ENVIRONMENTAL ENGINEERING**  
**HYDROLOGY AND HYDRAULIC ENGINEERING CHAIR**

**Watershed Hydrological Responses to Changes in Land Use and Land Cover at Hangar Watershed, Ethiopia.**

By

Abdata Wakjira Galata

A Thesis Submitted to School of Graduate Studies of Jimma University in Partial Fulfillment of the Requirements for the Degree of Master of Science in Hydraulic Engineering.

Advisor: - Dr. - Ing Tamene Adugna

Co-Advisor: - Mr. Megersa Kebede

January, 2019

Jimma, Ethiopia

## DECLARATION

I hereby declare that the Thesis entitled “**Watershed Hydrological Responses to Changes in Land Use and Land Cover at Hangar Watershed, Ethiopia**” is my original work, which I submit for partial fulfillment of the degree of Master of Science in Hydraulic Engineering to school of graduate studies, Hydrology and Hydraulic Engineering Chair, Jimma Institute of Technology, Jimma University. The Thesis conducted under the guidance of a main advisor, Dr. Eng. Tamene Adugna, and co-advisor, Megersa Kebede (MSc.).

Abdata Wakjira \_\_\_\_\_  
Signature                  Date

Dr. Eng. Tamene Adugna  
(Main Advisor)

\_\_\_\_\_  
Signature                  Date

Mr. Megersa Kebede  
(Co-advisor)

\_\_\_\_\_  
Signature                  Date



**Dedication**

*This thesis is dedicated to my beloved Family!*

## ABSTRACT

*Land use/land cover change has been responsible for altering the hydrologic response of watersheds leading to impact stream flows. The various water resources project planning and implementation need the knowledge of factors influencing watershed hydrology. Therefore, this study analyzed the land use/land cover change from 1987 to 2017, and the effect these changes have had on the hydrology of the Hangar watershed, which is the tributary of the Didessa River Basin, Ethiopia. The study was accomplished through integrating ERDAS imagine (2015) software and the SWAT model. The land use/land cover data (Landsat-5 TM, Landsat-7 ETM+ and Landsat-8 OLI\_TIRS, for the year 1987, 2001 and 2017 respectively) acquired from the website of USGS. The ERDAS imagine (2015) software used to generate the land use/land cover maps through the Maximum Likelihood Algorithm of Supervised Classification. The results indicated that, cultivated land and built-up area expanded (by 23.7%, 6%, and 28.2%) and (by 22.2%, 19.3%, and 37.2%) for LULC of 1987-2001, 2001-2017 and 1987-2017 respectively. Whereas, there was a decrease in forest (by 20.4%, 15.1% and 32%), rangeland (by 28.1%, 12.6% and 37%), grassland (by 64.9%, 6.1% and 67%) and water body (by 1.9%, 53.8% and 55%) for LULC of 1987-2001, 2001-2017 and 1987-2017 respectively. In addition to the land use/land cover data, the input data used for the SWAT model simulation were the DEM data, soil data, and climatic data. Parameters sensitivity analysis, calibration and validation of the SWAT model carried out by the SWAT-CUP through SUFI-2 program. Sensitivity analysis has indicated that the curve number is the most sensitive parameter that could affect the hydrology of the watershed. The model calibrated and validated using measured streamflow data of 13 years (1990-2002) and 9 years (2003-2011) respectively. The SWAT model performs well for both calibration ( $R^2 = 0.87$ ,  $NSE = 0.82$  and  $PBIAS = +1.4$ ) and validation ( $R^2 = 0.89$ ,  $NSE = 0.88$  and  $PBIAS = +1.2$ ). The result after simulation indicated that the annual total water yield of the watershed decreased which is 790.26mm for LULC of 1987, 777.38mm for 2001 and 766.08mm for 2017. The annual simulated stream flow through the study period is increased for wet (by 3%, 4% and 7%) and short rainy season (by 2, 5% and 7%) whereas, decreased for dry season (by 2%, 1% and 2%) for LULCC of 1987-2001, 2001-2017 and 1987-2017 respectively. Unless the proper watershed resources management implemented, the increase in runoff has implication for increasing soil erosion and sedimentation. The increase of wet season flow may result flooding, and the reduction of dry season flow may affect water scheme practice. Therefore, curving the changes of LULC towards increasing vegetation cover is very necessary in order to reduce surface runoff that contribute to wet season flow and increase infiltration that supply groundwater from which dry season/baseflow is contributed.*

**Keywords:** Hangar Watershed, Land Use and Land Cover Change, ERDAS, SWAT model, SWAT-CUP.

## **ACKNOWLEDGMENT**

Above all my thanks is to creator and governor of the worlds, almighty God for helping me in all directions. All things planned and appeared by him; without him, not anything happened that has happened.

I sincerely thank my main advisor Dr.Ing Tamene Adugna and my co-advisor Mr. Megersa Kebede for their advice during the study and constructive comments on the manuscript. They read the whole work and identified things which need modification so that, targeted parts replaced with better ideas.

From the beginning of this work to its cover Dr.Ing Tamene Adugna paid attention to direction seek forwarded questions. Unless he took time and gave suggestions on reached steps of the work, there were things that seem straight but time-consuming.

Ideas that generated on each stage of the work both online and offline from Mr. Megersa Kebede, were very helpful. The direction of proceed gained from him with an appreciable face without tired.

I am grateful to the Ethiopian ministry of education for giving me the chance to study my masters in Hydraulic Engineering and supporting the research financially. I wish to acknowledge Ethiopian Road Authority for providing the financial support of offered courses. Jimma University, Jimma Institute of technology played an important role by scheduling and giving courses and facilitating pre-conditions to collect the fund provided for this study.

The moral and strength gained from idea brow and pray of my family during up and down through my study period were unforgettable.

Finally, I have a special appreciation to my colleagues for their valuable suggestions and material support in order to accomplish this research.

# TABLE OF CONTENTS

Table of Contents	Pages
<b>ABSTRACT</b> .....	<b>IV</b>
<b>ACKNOWLEDGMENT</b> .....	<b>V</b>
<b>TABLE OF CONTENTS</b> .....	<b>VI</b>
<b>LIST OF TABLES</b> .....	<b>IX</b>
<b>LIST OF FIGURES</b> .....	<b>X</b>
<b>ACRONYMS</b> .....	<b>XII</b>
<b>1. INTRODUCTION</b> .....	<b>1</b>
1.1. Background.....	1
1.2. The Statement of problem.....	2
1.3. Objectives of the study.....	3
1.3.1. General objective .....	3
1.3.2. Specific objective.....	3
1.4. Research questions.....	4
1.5. Significance of the study.....	4
1.6. Scope of the study.....	4
<b>2. LITERATURE REVIEW</b> .....	<b>6</b>
2.1. Land use and land cover change .....	6
2.2. Causes of land use and land cover changes .....	6
2.3. Impacts of land use and land cover changes on the Hydrological process .....	7
2.4. Land use and land cover change and its implication in Ethiopia.....	7
2.5. Satellite images .....	8
2.6. LULC classification by the ERDAS imagine software .....	8
2.7. Hydrologic models and their application to study the impact of LULCC .....	9
2.7.1. Hydrologic models.....	9
2.7.2. The application of Hydrologic models to evaluate the impact of LULC change 10	



2.8.	The SWAT model.....	11
2.9.	SWAT-CUP .....	12
<b>3.</b>	<b>MATERIALS AND METHODS.....</b>	<b>14</b>
3.1.	Description of the study area .....	14
3.1.1.	Location .....	14
3.1.2.	Geology.....	15
3.1.3.	Rainfall.....	16
3.1.4.	Temperature .....	16
3.2.	Materials used .....	17
3.3.	Methods.....	17
3.3.1.	Data collections and sources.....	18
3.3.2.	Data analysis and preparation .....	22
3.3.3.	Image classification .....	26
3.3.4.	Accuracy assessment .....	27
3.4.	Evaluation of the impacts of LULCCs on the hydrological process .....	29
3.5.	Hydrological components of the SWAT model.....	29
3.5.1.	The surface runoff Generation.....	30
3.5.2.	Evapotranspiration computation .....	30
3.5.3.	Groundwater .....	31
3.5.4.	Flow routing.....	31
3.6.	The Model Set-Up.....	31
3.6.1.	SWAT project set up.....	32
3.6.2.	Watershed delineation.....	32
3.6.3.	HRUs analysis.....	33
3.6.4.	Write input tables.....	36
3.6.5.	Edit SWAT input .....	36
3.6.6.	SWAT simulation .....	36
3.7.	The SWAT-CUP Model .....	36
3.7.1.	Parameter Sensitivity analysis .....	37

3.7.2. Uncertainty Analysis.....	37
3.7.3. Model calibration and validation .....	37
3.7.4. The model performance evaluation .....	38
<b>4. Results and Discussion.....</b>	<b>41</b>
4.1. Land use/land cover change assessment .....	41
4.1.1. Land use/land cover Classification accuracy assessment .....	41
4.1.2. Land use/land cover change.....	42
4.1.3. Land use/land cover Maps .....	43
4.1.4. LULC change analysis between 1987-2001, 2001-2017 and 1987-2017.....	44
4.2. Sensitivity analysis.....	46
4.3. Flow Calibration using SUFI-2 Algorithm.....	47
4.4. Flow Validation using SUFI-2 algorithm .....	50
4.5. Model performance evaluation .....	54
4.6. Hydrological impacts of land use/land cover changes at the study area.....	54
4.6.1. The impacts of land use/land cover change on water balance components.....	54
4.6.2. The impacts of land use/land cover change on the streamflow .....	56
<b>5. CONCLUSION AND RECOMMENDATION .....</b>	<b>59</b>
5.1. CONCLUSION.....	59
5.2. RECOMMENDATION .....	60
<b>REFERENCES.....</b>	<b>61</b>
<b>APENDICES .....</b>	<b>68</b>

## LIST OF TABLES

Table 3.1 Description of materials and tools used for the study.....	17
Table 3.2 The corresponding sensors of Satellite images with its bands and resolution.....	20
Table 3.3 The summary of satellite data used.....	20
Table 3.4 The classified land use/land cover of the study watershed with its SWAT code ....	27
Table 3.5 Slope classes and its area of coverage .....	35
Table 3.6 The reported performance ratings for R <sup>2</sup> , NSE and PBIAS for SWAT model .....	39
Table 4.1 Accuracy assessment of classified LULC of Hangar watershed in 1987.....	41
Table 4.2 Accuracy assessment of classified LULC of Hangar watershed in 2001 .....	41
Table 4.3 Accuracy assessment of classified LULC of Hangar watershed in 2017 .....	42
Table 4.4 Summary of areas of LULC of Hangar Watershed through 1987 to 2017.....	42
Table 4.5 Analysis of LULC change between 1987-2001, 2001-2017 and 1987-2017 .....	45
Table 4.6 The most sensitive parameters with its rank of sensitivity .....	47
Table 4.7 The impacts of LULCC of 1987-2001, 2001-2017 and 1987-2017 periods on water balance components.....	56
Table 4.8 The impacts of LULCC of 1987-2001, 2001-2017 and 1987-2017 periods on streamflow. ....	57

## LIST OF FIGURES

Figure 3.1 Location of the study area .....	15
Figure 3.2 Average monthly Rainfall of the study area.....	16
Figure 3.3 Average maximum and minimum temperature of the study area .....	17
Figure 3.4 DEM of the study area.....	19
Figure 3.5 Double mass curve for stations in the watershed .....	24
Figure 3.6 Subset images of (A) Landsat-5 (TM), (B) Landsat -7 (ETM+) and (C) Landsat- 8 (OLI_TIRS) .....	25
Figure 3.7 Flowchart of the Landsat image pre-processing and classification.....	28
Figure 3.8 Hangar Watershed .....	33
Figure 3.9 The SWAT LULC (A), Soil (B) and Slope (C) classes of Hangar Watershed .....	35
Figure 3.10 Flow chart of the research approach.....	40
Figure 4.1 Areas of land use /land cover change in 1987, 2001 and 2017 .....	43
Figure 4.2 Land use/land cover map of the study area in 1987, 2001 and 2017 .....	44
Figure 4.3 The analysis of Land use/land cover changes through 1987 to 2017 .....	46
Figure 4.4 Graph of simulated versus observed flow during calibration for LULC of 1987 ..	48
Figure 4.5 Hydrograph of Monthly simulated and observed flow during calibration for LULC of 1987 .....	48
Figure 4.6 Graph of simulated versus observed flow during calibration for LULC of 2001 ..	49
Figure 4.7 Hydrograph of Monthly simulated and observed flow during calibration for LULC of 2001 .....	49
Figure 4.8 Graph of simulated versus observed flow during calibration for LULC of 2017 ..	50
Figure 4.9 Hydrograph of Monthly simulated and observed flow during calibration for LULC of 2017 .....	50
Figure 4.10 Graph of simulated versus observed flow during validation for LULC of 1987 ..	52

Figure 4.11 Hydrograph of Monthly simulated and observed flow during validation for LULC of 1987 .....52

Figure 4.12 Graph of simulated versus observed flow during validation for LULC of 2001 .53

Figure 4.13 Hydrograph of Monthly simulated and observed flow during validation for LULC of 2001 .....53

Figure 4.14 Graph of simulated versus observed flow during validation for LULC of 2017 .54

Figure 4.15 Hydrograph of Monthly simulated and observed flow during validation for LULC of 2017 .....54

Figure 4.16 Comparison of water balance components for LULC of 1987-2001, 2001-2017 and 1987-2017 .....56

Figure 4.17 Comparison of simulated streamflow for LULCC of 1987-2001, 2001-2017 and 1987-2017 periods .....58

## ACRONYMS

95PPU	95 Percent Prediction Uncertainty
AOI	Area of interest
DEM	Digital Elevation Model
DMC	Double mass curve
ERDAS	Earth Resources Data Analysis System
ET	Evapotranspiration
ETM+	Enhanced Thematic Mapper Plus
FAO	Food and Agricultural Organization
GIS	Geographical Information System
GLUE	Generalized Likelihood Uncertainty Estimation
GPS	Global Positioning System
HRUs	Hydrological Response Units
ISODATA	Iterative Self-Organizing Data Analysis Techniques Algorithm
LULC	Land Use and Land Cover
LULCC	Land Use and Land Cover Change
MCMC	Mark chain Monte Carlo
MSS	Multi Spectral Scanner
MWIE	Ministry of Water, Irrigation, and Electricity
NMSA	National Metrological Service Agency
NSE	Nash Sutcliffe Efficiency
OLI_TIRS	Operational Land Imager and Thermal Infrared Remote Sensor
ParaSol	Parameter Solution
PET	Potential Evapotranspiration

SUFI2	Sequential Uncertainty Fittings 2
SWAT	Soil and Water Assessment Tool
SWAT-CUP	Soil and Water Assessment Tool-Calibration and Uncertainty Programs
TM	Thematic Mapper
USGS	United States Geographic Survey
UTM	Universal Transverse Mercator Coordinate System
WGEN	Weather Generator

# 1. INTRODUCTION

## 1.1. Background

The problem, which would follow the change and/or modification of the naturally existed land cover, is severe overall the world. The change of land use to the feature not suitable to the topography of the area and removal of land cover may result in hydrologic cycle disturbance. The study by Dwarakish and Ganasri (2015) showed that land use/land cover change affect the different hydrological components like; interception, infiltration, and evapotranspiration thereby influencing soil moisture content, runoff generation (both process and volume) and streamflow regimes. Land under little vegetative cover is subject to high surface runoff amounts, low infiltration rate, and reduced groundwater recharge. The reduced infiltration and groundwater supply, eventually, leads to lowering of water tables and intermittence of once-perennial streams. Climate models have even shown that land use and land cover change affects global precipitation and temperature patterns (Chase, 1999) which influences hydrological process.

The Land use and Land cover conversion, such as from forest to various land use types is a common experience in most areas of Eastern African countries including Ethiopia, were ranked as the highest in Africa at a rate of 0.94% (1990-2000) and 0.97% per year (2000-2005) due to increasing human and livestock population in protected areas (Garedew, *et al.*, 2009). In developing countries, which characterized by agriculture-based economies and rapidly increasing human population, land use and land cover changes are highly detected. Conversion of land, to feed and shelter, the growing human population has been one of the primary modes for human conversion and/or modification of the environment (Piao, 2007). As is the case in many other developing countries, most of the population of Ethiopia live in rural areas and depends directly on the land for their livelihood. This rural population is currently growing rapidly, and consequently inducing many effects on the resource base. As it stated by Bewket and Sterk (2004), one such effect is a very dynamic land use and land cover. Land use/land cover change largely affects the water balance mainly by changing the process of evaporation, transpiration, an interception, and surface runoff (Tekleab, *et al.*, 2014).



The spatial and temporal variability of watershed resources (particularly land cover change and climatic change) have a significant influence on the quantity and quality of river water flow (Tufa *et al.*, 2014). Many studies performed in different parts of the country, for instance, Solomon (2005) in Headstream of Abbay Watershed; Zeleke, and Hurni (2001) in northern Ethiopian highlands addressed a common concern as the water resource degradation brought about by the decrease in the area under natural vegetation and its conversion into other types of land use that are human-managed systems.

Conversion of natural vegetation cover to other land use types such as farmlands, grazing lands, human settlements, and urban center causes loss to biodiversity, deforestation and land degradation, which could disturb hydrologic cycle. The objective of this study is to evaluate the effects of land use/land cover change on the hydrological process of Hangar watershed. It could be the essential input for the development of effective and appropriate action for sustainable planning, implementing and management of natural water resources in the country in general and at the study area in particular.

## **1.2. The Statement of problem**

Human health and welfare, food security and industrial developments are dependent on adequate supplies of suitable water; however, water resources affected by many parameters (Kebede, *et al.*, 2014). Irrespective of Ethiopia possesses large sources of water; the sources not utilized with their possible capacity. Land use/land cover change is responsible for altering the hydrologic response of watersheds leading to affect the streamflow. With the fast-growing population, the uncontrolled agricultural activities to bring more land to agriculture have deteriorated the environment (Tekle and Hedlund, 2000). Vegetation losses, consequent runoff increase, and a decrease in infiltration reduce water tables, leading to situations of below optimal baseflow recharge during the dry season.

The performed studies about the factors that could affect the hydrological process at the watershed level are not much as in largest basins of the country. As Miheretu and Yimer (2017) stated, studies of LULC dynamics at subwatershed level are rare in Ethiopia. To estimate and predict the demands for different water resources schemes, enough studies should carried out about the factors affecting the watershed. However, no study carried out about factors that

affect hydrology of the watershed behavior and their relation to land use/land cover changes of Hangar Watershed; which can be a relevant consideration in the design of integrated watershed management and of appropriate sustainable land management practices, strategies and policies. To predict the future effects of land use and land cover change on the streamflow, it is important to have an understanding of the effects a historic LULCC have had on the hydrological process. From the overview of the study area, it observed that the area under the coverage of natural vegetation was reducing due to expansion of farmland and settlements. Since the study watershed is located in agricultural area the change in land use and land cover continued unless the factors facilitating these changes identified and measures need to be taken is recommended. However, at the study area no software based land use and land cover change determination was carried out. Since the change in land use and land cover is not identified by the study, the hydrological responses of the watershed was not evaluated. To fill this gap ERDAS imagine 2015 software was used to investigate the changes in land use and land cover and the hydrological responses of the watershed was evaluated by using SWAT model 2012.

### **1.3. Objectives of the study**

#### **1.3.1. General objective**

The general objective of this study is to evaluate the Hydrological impacts of Land Use/Land Cover Changes in the Hangar Watershed.

#### **1.3.2. Specific objective**

The study carried out to fulfill three specific objectives:

- ❖ To analysis of the changes in the land use/land cover of the Watershed for different specified periods.
- ❖ To characterize and evaluate the performance of the SWAT model.
- ❖ To evaluate the responses of streamflow to changes in land use/land cover of the Watershed so that, measures could be taken to reduce the influence of LULCC on it.

#### **1.4. Research questions**

The following are questions asked to answer the specific objectives mentioned above.

- ❖ What is the trend of land use/land cover in the Watershed for the specified periods?
- ❖ Which parameters are the most sensitive and how does the SWAT model perform for the Hangar watershed under land use/land cover changes of different periods?
- ❖ What is the response of the streamflow of the watershed to changes in land use/land cover and what measures need to be taken?

#### **1.5. Significance of the study**

The knowledge of how land use and land cover change influences watershed hydrology could enable local governments and policy makers to plan and employ appropriate response strategies to minimize the undesirable effects of future land use/land cover change or modifications on the hydrological process. Various water resources projects planning and implementation requires knowledge of the extent of land use and land cover changes on watershed hydrology.

This study expected to help concerned sectors in planning, implementing and managing water resource projects in the study area and be an input for those who are interested in further research in related field and area of study. Since most part of the study watershed is located in the rural agricultural area, farmers could play important role to minimize the changes in land use and land cover if they gained awareness of its impacts. Therefore, understanding the changes in the land use/land cover and its impact on the yield from the land and on the hydrological process helps the concerned body to give awareness for farmers thereby, sound policies would formulated and implemented to minimize undesirable future impacts and devise management alternatives.

#### **1.6. Scope of the study**

This study is geographically limited to Hangar River watershed, the tributary of Didessa River basin, Ethiopia. Within the time provided for this study, the objectives set addressed and the asked research questions answered. The land use and land cover change that expected to take place in the Hangar River watershed was reached by integrating software and hydrologic

models and the effect of these changes on the hydrological process of the watershed was discussed.

## **2. LITERATURE REVIEW**

### **2.1. Land use and land cover change**

According to the studies, Klepeis and Turner (2001) jointly initiated in 1999 by the International Geosphere-Biosphere Program (IGBP) and the International Human Dimension Program on Global Environment Change (IHDP), Land use refers to the arrangements, activities, and inputs undertaken in a certain land cover type by human actions for social and economic purposes of which land managed. Whereas, the Land cover is the physical and biophysical cover of the earth's surface and immediate subsurfaces like vegetation, water, desert, ice etc.

Land Use and Land Cover Changes (LUCCs) is the shift in intent and/or management constitutes land use and land cover. The two forms through which Land Use and Land Cover change occur are land use/land cover conversion and land use/land cover modification (Lambin *et al.*, 2003). Land use and land cover conversion refer to change from one cover or use type to another, as is the case in agricultural expansion, deforestation, or change in urban extent. Land use and land cover modification, on the other hand, involves the maintenance of broad cover or use type in the face of change in its attributes. Both conversion and modifications of land use and land cover have important environmental consequences through their impacts on soil, water, biodiversity, and microclimate, and hence, contribute to watershed degradation (Tufa *et al.*, 2014).

### **2.2. Causes of land use and land cover changes**

A number of natural and human driving forces causes Land cover changes. The effects of human activities are immediate and often radical; whereas, natural effects such as climate change are felt only over a long period of time results in a decrease of evapotranspiration and water recycling that causes a reduction in a rainfall, (Bewket, 2002). Destructive land use change may also affect the hydrological cycle either through increasing the water yield during the wet season or through diminishing or even eliminating the low flow during the dry season in certain circumstances. The central theme in land use/land cover change (LULCC) issues is the interaction between human beings and the environment they live in. Land use/land cover

change has a direct relationship with the productivity of the land and biological diversity in protected areas.

As a result, identifying the root causes of LULCCs and monitoring its dynamics and impact is critical to environmental sustainability efforts (Belay *et al.*, 2014). According to Miheretu and Yimer (2017), socio-economic and biophysical variables act as the driving forces of land use changes. Driving forces generally subdivided into two groups: proximate causes and underlying causes. Proximate causes are the activities and actions that directly affect land use like wood extraction or road building. Underlying causes are the fundamental forces that underpin the proximate causes, including demographic, economic, technological, institutional and cultural factors.

### **2.3. Impacts of land use and land cover changes on the Hydrological process**

Land use/land cover is a biophysical feature that has strong interrelation between atmosphere and ground surface hydrologic cycle. Both climate and land use and land cover change have great influence on the hydrological response of a watershed (Dwarakish and Ganasri, 2015). Land use changes in a watershed can influence water supply by altering hydrological processes such as infiltration, groundwater recharge, base flow and runoff (Lin *et al.*, 2007). Its influence is direct on climate and water resources on the ground. Land under little vegetation cover (Bewket, 2002), is subjected to high surface runoff, low water retention and low infiltration rate. Human-induced land use changes such as deforestation, afforestation, and agricultural and urban development within the river basin can affect the hydrological cycle (Babar and Ramesh, 2015). Increasing forest cover would substantially reduce sediment yield and modulate streamflow. The surface flow of watershed hydrology can be influenced by interactions between environmental conditions such as land use/land cover change (LULCC) and climatic characteristics (Kebede *et al.*, 2014).

### **2.4. Land use and land cover change and its implication in Ethiopia**

In Ethiopia, land use can be seen from the perspective of human activities such as agriculture, building construction and urbanization, which has led to the increased human population within urban areas and depopulation of rural areas (Hamza and Iyela, 2012). As studies carried out in different parts of Ethiopia for instance; in West Ethiopia (Solomon, 1994); in North-

Western Ethiopia (Zelege and Hurni, 2001); in North Ethiopia (Tegene, 2002); in North-Eastern Ethiopia (Girmay, 2003); in South-Western Ethiopia (Denboba, 2005); and in North Ethiopia (Solomon, 2005) showed that croplands have expanded at the expense of natural vegetation, including forests and shrublands. The mean monthly discharge for wet months had increased while it decreased during dry season due to the land use/land cover change in Hare River Watershed (Tadele and Förch, 2007) and in Abay/Upper Blue Nile basin (Tekleab *et al.*, 2014). From these studies, it understood that the components of the hydrologic cycle, which are responsible to influence streamflow, affected due to the expense of natural vegetation.

## **2.5. Satellite images**

The satellite sensors acquire images of the earth's surface without contact with it, which helped to classify the type of land cover and land uses (Irons, *et al.*, 2012). The operational Landsat satellites with four different sensors were available through the United States Geological Survey (USGS) Center. The MSS (multispectral scanner) sensor on the Landsat-1-4 satellite provide the oldest and lowest quality of Landsat data, from 1972 to 2013, the TM (thematic mapper) sensor on the Landsat-5 satellite and the ETM+ (enhanced thematic mapper plus) sensor on the Landsat-7satellite provides improved quality of Landsat data from 1982 to 2011 and 1999 to present respectively (<https://www.earthexplorer.usgs.gov/>). Data from the two sensors, TM and ETM+ can be used to measure and monitor the same landscape phenomena and that Landsats 5 and 7 data can use interchangeably with proper caution (Vogelmann *et al.*, 2001). The OLI\_TIRS (Operational Land Imager and Thermal Infrared Remote Sensor) on the Landsat-8 satellite provide the best quality of all, from 2013 to present (Blackett, 2014). The strength of the Landsat-8 OLI dataset is crucial especially in sub-Saharan Africa where high-resolution remote sensing data availability remains a challenge (Dube and Mutanga, 2015).

## **2.6. LULC classification by the ERDAS imagine software**

The Earth Resources Data Analysis System (ERDAS) imagine software is a powerful tool for studying geographic data quickly and accurately (Long and Srihann, 2004). It uses the spectral information represented by the digital numbers in one or more spectral bands to assign all pixels in the image to a particular classes or themes. The ERDAS imagine uses two approaches in image classification: Per-pixel and Object-oriented classification (Guide, 2010). In per-pixel

classification, the algorithm categorizes each input pixel into a spectral feature class based solely on its individual multispectral vector (signature). Object-oriented classification-the input pixels grouped into spectral features (objects) using an image segmentation algorithm.

The three common per-pixel methods are supervised classification, unsupervised classification and rule-based classification (Long and Srihann, 2004). Supervised classification-the analyst supervises the categorization of a set of specific classes by providing training statistics that identify each category. Unsupervised classification-the raw spectral data are grouped first, based solely on the statistical structure of the data. Rule-based classification-spectrally categorized pixels are classified using ancillary data in a GIS model.

## **2.7. Hydrologic models and their application to study the impact of LULCC**

### **2.7.1. Hydrologic models**

A watershed hydrology model is a model used to simulate hydrologic processes of the watershed under different circumstances expected to affect the hydrology of the watershed. As it stated by Singh and Woolhiser (2002), the model structure and architecture determined by the objective for which the model is built. However, as the study by Mengistu (2009) indicated, hydrologic models, in general designed to meet one of the two primary objectives. One objective of watershed modeling is to gain a better understanding of the hydrologic processes in a watershed and of how changes in the watershed may affect these phenomena. According to this study, another objective of watershed modeling is the generation of synthetic sequences of hydrologic data for facility design or for use in forecasting.

Depending upon the way the hydrologic models treat the randomness, space and time variability of hydrologic phenomena processes, models classified as deterministic, stochastic, or mixed. In a deterministic model, outcomes are precisely determined through known relationships among states and events, without any room for random variation. In such models, two equal sets of input always yield the same output if run through the model under identical conditions. On the other hand, if a model has at least one part of the random character that is not explicit in the model input, but only implicit or hidden it called stochastic model. If a mix of deterministic and stochastic components describes the model components, the model called stochastic-deterministic or hybrid model (Van Liew, *et al.*, 2007). Vast majorities of the



models are deterministic, and virtually no model is fully stochastic. Based on process description, the deterministic hydrological models can be classified into three main categories: lumped models, distributed models, and semi-distributed models. Parameters of lumped hydrologic models do not vary spatially within the basin and thus, basin response is evaluated only at the outlet, without explicitly accounting for the response of individual sub-basins. The parameters often do not represent physical features of hydrologic processes and usually involve a certain degree of empiricism. As it is addressed by Beven (2001), most of such models are not capable of representing all hydrologic processes for investigating the impacts of land use and climate change on the hydrological regime.

Distributed models on the other hand fully permit parameters to vary in space at a resolution usually chosen by the user. Distributed modeling approach attempts to incorporate data concerning the spatial distribution of parameter variations together with computational algorithms to evaluate the influence of this distribution on simulated precipitation-runoff behavior (Van Liew and Garbrecht, 2003). These models generally require large amounts of (often-unavailable) data for parameterization in each grid cell.

Semi-distributed (simplified distributed) models partially allow parameters to vary in space by categorizing the basin into a number of smaller sub-basins. The main merit of these models is that their structure is more physically based than the structure of lumped models and that they are less demanding on input data than fully distributed models. SWAT, HEC-HMS, HSPF, PRMS, DWSM, TOPMODEL, and HBV are considered as semi-distributed models (Mengistu, 2009).

### **2.7.2. The application of Hydrologic models to evaluate the impact of LULC change**

Specifically, LULCC information is of critical importance in hydrologic modeling, as it helps to determine model variables that account for the volume, timing, and quality of runoff (Gashaw *et al.*, 2018). The method to evaluate the impacts of land use and land cover changes, land management practices and climate change on hydrological regimes can be achieved by integrating GIS, remote sensing, and hydrological models (Mtalo *et al.*, 2012). To contribute to the planning and management of available land resources, especially in the watersheds

where other kinds of background data are often lacking, LUCCs can deliver by using satellite images (Moran *et al.*, 2001).

Even though there are no clear guidelines for model selection, the study by Shen and Phanikumar (2010) showed that, the model functionality and complexity can become criteria's in model selection. The model functionality differs in terms of hydrologic process representation, the equations developed to simulate these processes and model discretization. In addition, model complexity can be defined by the estimated data, resources, time, and cost that are required to parameterize and calibrate a model, as well as the professional judgment and experience required to operate these models (Shen and Phanikumar, 2010).

Beginning from the studied physical system, the first step is to define the problem and determine what information needed and what questions need to be answer (Abushandi and Merkel, 2013). It is necessary to evaluate the required output, the hydrologic processes that need to be model and availability of input data. The selection of a particular model is a key issue to get satisfactory answers to a given problem. In particular, it is necessary to identify the simplest model that will yield adequate accuracy, bearing in mind that model complexity is not synonymous with the accuracy of the results (Singh, and Woolhiser, 2002). The model has to be characterize by flexibility, by the possibility of making it applicable under various spatial and temporal conditions and that increased accuracy has to be worth the increased effort (Mengistu, 2009). For this study, a physically based semi-distributed hydrological model (SWAT) that allows several different subunits or objects to be define within a watershed (Neistch, *et al.*, 2011) was utilized. For economically poor countries like Ethiopia, the data requirements of this model acquire from second sources.

## **2.8. The SWAT model**

The SWAT (Soil and Water Assessment Tool) model is semi-distributed physically based simulation model and can predict the impact of land cover change and land management practices on hydrological regimes in watersheds with varying land cover, soils, and management conditions over long periods (Arnold *et al.*, 2012). The major model components include weather, hydrology, erosion/sedimentation, plant growth, nutrients, pesticides, and land management. The model operates on a daily time step, allows a basin to subdivide into

natural sub-watersheds, and characterized by its focus on land management, water quality loadings, and continuous simulation over long time spans (Van Liew and Garbrecht, 2003). In SWAT model, the impacts of spatial variations in topography, land use, soil and other watershed characteristics on hydrology considered in subdivisions (Mengistu, 2009). The model calculations performed on HRU basis and flow and water quality variables routed from HRU to sub-basin and subsequently to the watershed outlet (Singh, and Woolhiser, 2002).

A watershed is divided into a number of sub-watersheds based upon drainage areas of the tributaries and each sub-watershed is further divided into a number of Hydrologic Response Units (HRUs) based on land use and land cover, soil and slope characteristics. Among the many advantages of this model are; it has incorporated several environmental processes, it uses readily available inputs, it is user-friendly, it is physically based and semi-distributed, and it is computationally efficient to operate on large watersheds in a reasonable time (Arnold, *et al.*, 2012).

## **2.9. SWAT-CUP**

The SWAT-CUP (SWAT-Calibration and Uncertainty Programs) is a computer program developed for the calibration and uncertainty analysis of the SWAT model (Vilaysane *et al.*, 2015). It enables sensitivity analysis, calibration, and validation of the SWAT model through procedures embedded to it. The SWAT-CUP linked to five different algorithms such as Sequential Uncertainty Fitting SUFI-2, Particle Swarm Optimization, (POS), Generalized Likelihood Uncertainty Estimation (GLUE), Parameter Solution (ParaSol), and Mark chain Monte Carlo (MCMC) (Abbaspour *et al.*, 2004).

GLUE is an uncertainty analysis technique inspired by importance sampling and regional sensitivity analysis (Yang *et al.*, 2008). Disaggregation of the error into its source components is difficult, particularly in cases common to hydrology where the model is non-linear and different sources of error may interact to produce the measured deviation (Mirzaei *et al.*, 2015). In ParaSol technique the simulations performed are divided into “good” simulations and “not good” simulations by a threshold value of the objective function (Yang *et al.*, 2008). MCMC methods are a class of algorithms for sampling from probability distributions based on

constructing a Markov chain that has the desired distribution as its equilibrium distribution (Yang *et al.*, 2008).

In SUFI-2, parameter uncertainty is described by a multivariate uniform distribution in a parameter hypercube, while the output uncertainty is quantified by the 95% prediction uncertainty band (95PPU) calculated at the 2.5% and 97.5% levels of the cumulative distribution function of the output variables (Abbaspour *et al.*, 2007). Parameter uncertainty accounts for all sources of uncertainty, i.e., input uncertainty, structural uncertainty, parameter uncertainty and response uncertainty (Beven and Freer, 2001). The degree to which all uncertainties are accounted for and the strength of a calibration/uncertainty analysis are quantified by the P-factor which is the percentage of measured data bracketed by the 95% prediction uncertainty (95PPU) and R-factor respectively which is the average thickness of the 95PPU band divided by the standard deviation of the measured data (User Manual, 2014). The value for P-factor ranges between 0 and 100%, while that of R-factor ranges between 0 and infinity. A P-factor of approaches to one and R-factor of approaches to zero indicates a simulation that corresponds to measured data (User Manual, 2014). SUFI-2 allows its users several choices of the objective function for instance, the coefficient of determination ( $R^2$ ) and Nash-Sutcliffe efficiency (NSE) (Abbaspour *et al.*, 2004). For this study, SUFI-2 technique that perform parallel processing (calibration and uncertainty analysis) is selected.

### **3. MATERIALS AND METHODS**

#### **3.1. Description of the study area**

##### **3.1.1. Location**

Hangar River watershed is located in west-central Ethiopia. The River emerges from Horo Guduru Wollega zone near Jardaga Jarte district and it flow south-west to join Didessa River, which is a tributary of the Blue Nile (also called the Abbay River basin in Ethiopia). Hangar enter the Didessa approximately halfway between the town of Nekemt and the village of Cherari at a latitude and longitude of 9°35'N and 36°2'E respectively. It has a number of tributaries that cover an area of nearly 7673.87km<sup>2</sup>. The topography or elevation of the watershed ranges from 844 to 3207 m above mean sea level. Generally, the Hangar River watershed is geographically located between 36 ° 31 ' 41'' to 37 ° 06 ' 50'' East longitude and 9 ° 41 '58'' to 9° 59 ' 56''North Latitude.

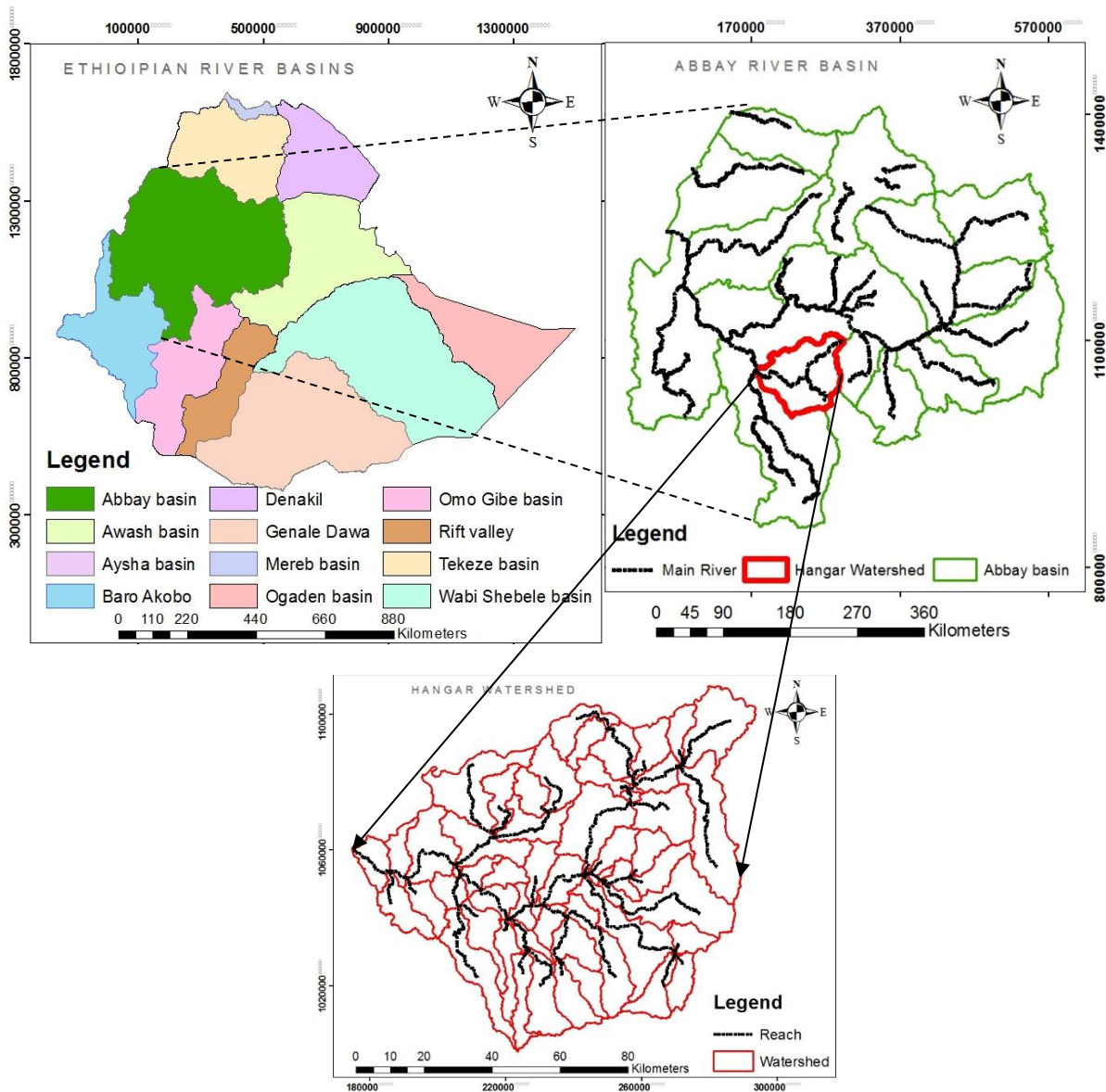


Figure 3.1 Location of the study area

### 3.1.2. Geology

The regional geology of the study area developed from three types of geological terrains. These are Quaternary sediments, Paleozoic to Mesozoic rock, Precambrian rock (from youngest to oldest). Most of the study area is covered with intrusive Precambrian rocks mainly granite with coarse-grained texture and massive in nature which is overlaid by thick black to brownish cotton soil (OWWDSE, 2015).

### 3.1.3. Rainfall

Climatic elements like rainfall, temperature, relative humidity, sunshine, and wind can affect by geographic location and altitude. As per the data collected from the National Metrological Service Agency (NMSA), the study area receives heavy rainfall from June to September and experiences a limited amount of rainfall for the left seven months. Figure 3.2 shows the average monthly rainfall of used stations for this study.

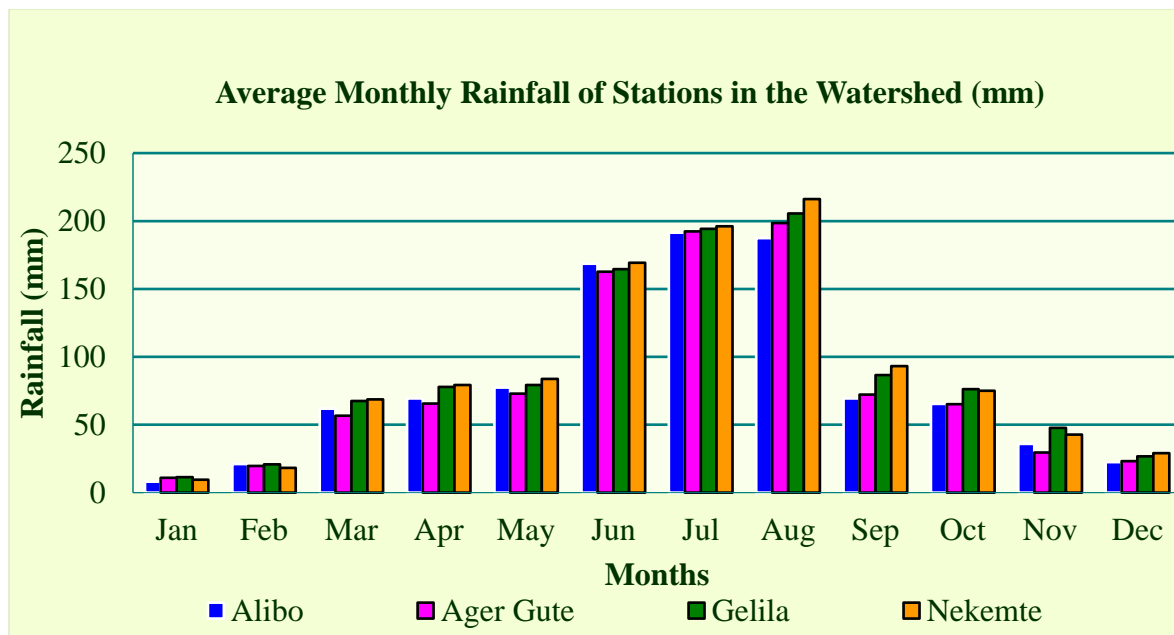


Figure 3.2 Average monthly Rainfall of the study area

### 3.1.4. Temperature

In the study area, the average maximum temperature experienced in the months of February, March, and April whereas, the average minimum temperature occurred in the months of September, October and November. Average maximum and a minimum temperature of Nekemt station are shown in Figure 3.3 of below and see for others (Appendix C).

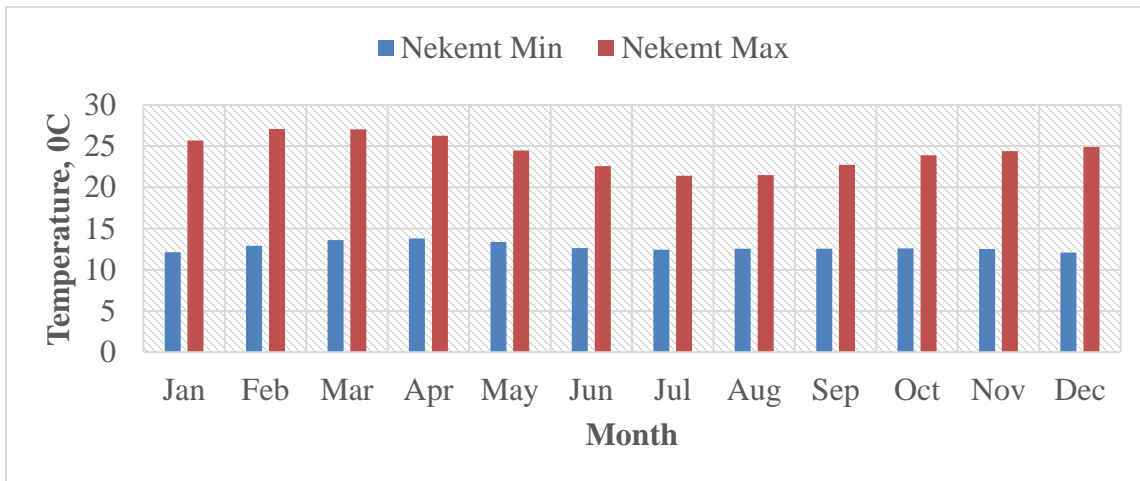


Figure 3.3 Average maximum and minimum temperature of the study area

### 3.2. Materials used

The materials used for this study with the corresponding purposes it provided are shown in Table 3.1.

Table 3.1 Description of materials and tools used for the study

Materials/Tools	Its Uses
Arc GIS 10.3	To arrange spatial data and prepare their map
Arc SWAT 2012	To delineate watershed and simulate hydrological parameters of the watershed
ERDAS imagine 2015	For Landsat image process, image classification and accuracy assessment
PCP STAT	To calculate statistical parameters of daily precipitation data used in the weather generator
DEW02	To calculate the average daily dew point temperature per month
SWAT-CUP	To calibrate and validate SWAT output
XLSTAT 2018	For filling of missed data
GPS	For data collection on the field
Google Earth	To provide recent information on watershed's LULC

### 3.3. Methods

The procedures followed to accomplish the study are discussed under the following sub-topics starting from data collection to analysis of the impact of Land use and land cover change on hydrological process.



### **3.3.1. Data collections and sources**

Dataset was collected from primary and secondary sources. Primary data are the ground truth data about the LULC and gained from the study area by using different methods such as; interviewing with those who are living at the site, discussing with others who have information about the field and collected with GPS for the recent period during field observation. Whereas, secondary data are recorded data, collected from different sources. These data are: weather data that collected from National Meteorological Service Agency (NMSA) of Ethiopia, land use and land cover data that acquired from U.S Geographic Survey, soil data which collected from GIS department of ministry of Water, Irrigation and Electricity (MoWIE), the streamflow data that gained from the hydrology department of the ministry of Water, Irrigation and Electricity (MoWIE) and Topographic data (DEM) which was acquired from the website of Alaska satellite facility (<https://www.asf.alaska.edu/sar-data/palsar/>). The analysis of collected data carried out before using it.

#### **3.3.1.1. Digital Elevation Model (DEM)**

Digital Elevation Model (DEM) was the first inputs of the SWAT model. The type of DEM used for the SWAT model in this study was 12.5 by 12.5m resolution DEM that downloaded from the website of Alaska satellite facility (<https://www.asf.alaska.edu/sar-data/palsar/>). Using 12.5 by 12.5m DEM was advantageous to show smaller streams clearly during watershed delineation. Since the study area could not be covered with one image, more images downloaded and mosaicked with the aid of Arc GIS before extracting the area of interest. The DEM was used for determination of flow direction and flow accumulation calculation, drainage network generation, watershed delineation, sub-basin definition, and HRUs setup. The topographic parameters of the studied watershed such as terrain slope, channel slope or reach length were also derived from Digital Elevation Model (DEM). Based on the topographic characteristics and area of the watershed, the SWAT model had identified 61 sub-basins in the studied watershed. The DEM of the studied watershed is shown in Figure 3.4.

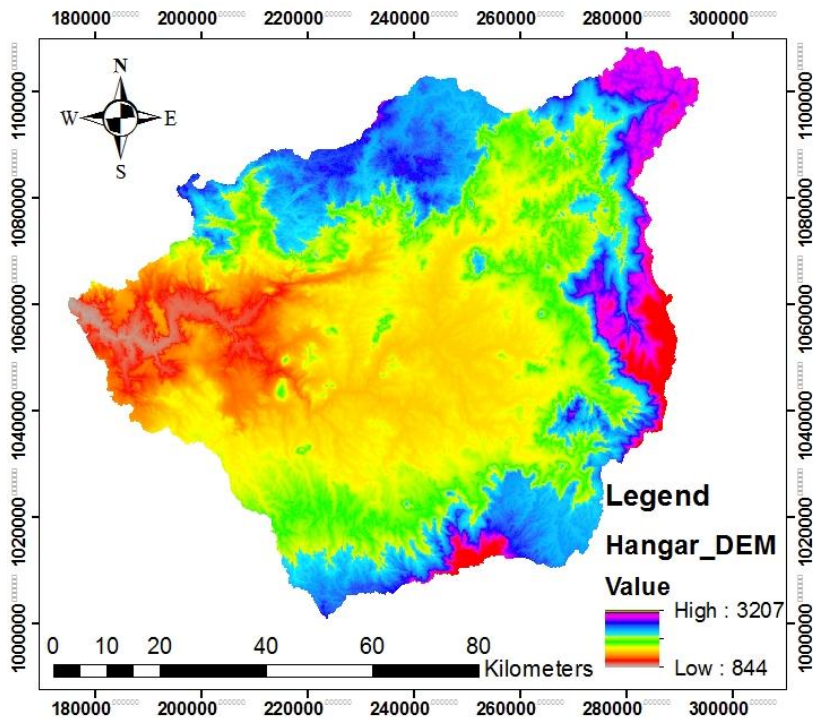


Figure 3.4 DEM of the study area

### 3.3.1.2. Land use/land cover

Land use/land cover data is the essential input in hydrological models because; it largely affects the water balance mainly by changing the process of evaporation, transpiration, interception and surface runoff (Tekleab, *et al.*, 2014). Landsat images collected with zero cloud cover from the USGS center (<https://www.earthexplorer.usgs.gov/>). As much as possible the acquisition dates of the obtained Landsat data made in the same season of the years to minimize the impacts of a seasonal variation in vegetation pattern and distribution throughout the year.

The images were identified by the Landsat grid describing path (p) and row (r) for which the Hangar watershed is covered with 170 paths and 53 to 54 rows. Landsat-5 TM sensor, Landsat-7 ETM+ sensor, and Landsat-8 OLI\_TIRS sensor have 7, 8 and 11 bands respectively. For TM and ETM+ sensors, bands (1-5 and 7) have a spatial resolution of 30m. The band 6 of TM sensor has a spatial resolution of 120m. Bands of (6.1 and 6.2) for Landsat-7 ETM+ sensor have 60m spatial resolution (Moran *et al.*, 2001). OLI and TIRS on Landsat-8 will coincidentally collect data and the observatory will transmit the data to the ground system where it will be archived, processed to Level 1 data products containing well calibrated and co-registered OLI

and TIRS data, and made available for free distribution to the general public (Iros *et al.*, 2012). One sensor, the Operational Land Imager (OLI), will collect image data for nine shortwave spectral bands over a 185 km swath with a 30 m spatial resolution for all bands (1-7, 9) except a 15 m panchromatic band (band 8). The other instrument, the Thermal Infrared Remote Sensor (TIRS), will collect image data for two thermal bands (10 and 11) with a 100 m resolution over a 185 km swath (Blackett, 2014). Both sensors offer technical advancements over earlier Landsat instruments (Iros *et al.*, 2012). The summary of bands with its respective spatial resolution for the three sensors are shown in Table 3.2.

Table 3.2 The corresponding sensors of Satellite images with its bands and resolution

Sensor	Bands	Resolution
TM	1-5,7	30m
	6	120m
ETM+	1-5,7	30m
	6.1 and 6.2	60m
	8	15m
OLI	1-7,9	30m
	8	15m
TIRS	10 and 11	100m

For this study, the Landsat imageries, Landsat-5 Thematic Mapper for 1987, Landsat-7 Enhanced Thematic Mapper plus for 2001 and Landsat-8 Operational Land Imager and Thermal Infrared Remote Sensing for 2017 were used. The summary of sensor type, path and row, spatial resolution, their acquisition date, producer and the bands of the satellite data used for this particular study are shown in Table 3.3.

Table 3.3 The summary of satellite data used

Year	Sensor	Bands	Spatial Resolution	Path_Row	Producer	Acquisition Date
1987	TM	1-5,7	30m	170_053	USGS	22/1/1987
	TM	1-5,7	30m	170_054	USGS	22/1/1987
2001	ETM+	1-5,7 and 8	30m and 15m	170_053	USGS	5/2/2001
	ETM+	1-5,7 and 8	30 and 15m	170_054	USGS	5/2/2001
2017	OLI	1-7,9 and 8	30m an 15m	170_053	USGS	8/1/2017
	OLI	1-7,9 and 8	30m an 15m	170_054	USGS	8/1/2017

### **3.3.1.3. Soil**

To account the soil properties in the model, a soil map of Abay River basin was obtained from the GIS department of MoWIE and that of the study area was clipped from it by Arc GIS. There are 8 soil types in the study watershed. They are: Haplic Alisols (38.14%), Eutric Leptosols (2.37%), Haplic Nitisols (3.6%), Eutric Vertisols (0.1%), Dystric Leptosols (12.94%), Haplic Acrisols (26.84%), Rhodic Nitisols (16.0%) and Haplic Arenosols (0.01%) (Figure 3.9). To integrate the soil map with the SWAT model, a soil database containing physical and chemical properties of soils was prepared for each soil layer and added to the SWAT soil databases.

### **3.3.1.4. Climate**

SWAT requires long-term daily climate data. Therefore, daily climate data for the periods 1987 to 2017 obtained from the Ethiopian National Meteorological Service Agency (NMSA). For this study, the data of four stations within the watershed were used. Among these stations depending on the direction of Flow of the River Alibo represents stations located at the upstream of the Hangar River, Gelila represents stations flowing from the right-hand side of the river, Nekemte represents stations from left-hand side and Anger Gute represents stations located at the mid downstream of the river. The mean monthly rainfall and temperature (1987–2017) characteristics of the stations are shown in Figure 3.2, 3.3 Appendix D.

### **3.3.1.5. Streamflow**

The raw data of streamflow obtained from the hydrology department of MoWIE. The gauging station of the collected streamflow data was not at the exact confluence point of the Hangar River, which need transferring the gauged data to the area of interest/outlet. The formula to transfer gauged discharge to ungauged site of interest developed by Dr. Admasu Gebeyehu (Gebeyehu, 1989) which works for sites within the same hydrologic region, and there are no major tributaries or diversions between the gauge and the site of interest. However the formula was developed 29 years ago, during which availability of another technology was rare. Today these difficulties are overcome by the found better technologies. Therefore, for this study the problem is solved by the model itself. The model calibrated at the gauging station and simulated at the outlet of the watershed.

### 3.3.2. Data analysis and preparation

The collected and acquired data were analyzed and prepared before any use through the approaches below.

#### 3.3.2.1. Filling missing weather data

SWAT model needs full daily weather data to analysis and generate the result. The data collected from the National Metrological Service Agency have much-missed data. The missed daily rainfall and temperature data filled by Xlsat 2018 program, where multiple leaner regression used to fill missed daily rainfall data from neighboring station and missed maximum and minimum daily temperature data were filled by average multiple imputation methods.

Since the SWAT model requires solar radiation in day, the sunshine hour data of Nekemt station collected from NMSA was converted to solar radiation by using empirical equation developed by Angstrom (Equation [3.2]). The Angstrom–Prescott equation (Prescott, 1940) related Extraterrestrial radiation to solar radiation in a given location and average fraction of possible sunshine hours by equation [3.2] (Muzathik *et al.*, 2011).

$$R_s = \left[ a + b \left( \frac{n}{N} \right) \right] * R_a \quad [3.2]$$

Where  $R_s$  is the solar or short wave radiation,  $R_a$  is the extraterrestrial radiation,  $n$  is the actual duration of sunshine [hour],  $N$  is the maximum possible duration of sunshine or daylight hours [hour],  $\frac{n}{N}$  is relative sunshine duration [-], and  $a$  and  $b$  are empirical coefficients, expressing the fraction of extraterrestrial radiation reaching the earth on overcast days ( $n = 0$ ) and  $a + b$  fraction of extraterrestrial radiation reaching the earth on clear day ( $n = N$ ).  $N$  and  $R_a$  are computed by equation (3.3) and (3.4).

$$N = \frac{24 * \omega_s}{\pi} \quad [3.3]$$

$$Ra = \frac{24(60)}{\pi} * G_{SC} * d_r [\omega_s \sin \varphi \sin \delta + \cos \varphi \cos \delta \sin W_s] \quad [3.4]$$

Where  $Ra$  is extraterrestrial radiation ( $\text{MJm}^{-2}\text{day}^{-1}$ ),  $G_{SC}$  is solar constant =  $0.0820\text{MJm}^{-2}\text{min}^{-1}$ ,  $d_r$  is inverse relative distance Earth-sun,  $\varphi$  is latitude of the site (rad),  $\delta$  solar declination (rad) and  $\omega_s$  sunset hour angle (rad).

Allen *et al.*, (1998) suggested the value of  $a = 0.25$  and  $b = 0.5$  and as the inverse relative distance Earth-sun,  $d_r$ , Latitude of the site,  $\varphi$  and the solar declination,  $\delta$  are calculated by the equation (3.5), (3.6) and (3.7).

$$d_r = \left[ 1 + 0.033 \cos \left( \frac{2\pi J}{365} \right) \right] \quad [3.5]$$

$$\varphi = Lat * \frac{\pi}{180} \quad [3.6]$$

Where *Lat*- Latitude in degree

$$\delta = 0.409 \sin \left[ \frac{2\pi J}{365} - 1.39 \right] \quad [3.7]$$

Where  $J$  is the number of the day in the year between 1 (1 January) and 365 or 366 (31 December). The Sunset hour angle,  $\omega_s$  could be computed from the equation (3.8).

$$\omega_s = \cos^{-1} [-\tan(\varphi)\tan(\delta)] \quad [3.8]$$

### 3.3.2.2. Checking consistency of weather data

Inconsistency of climatic data could be happen during record because of changes in conditions during record, changes in instrumentation, changes in gauge location, changes in observation practices etc. Before using any weather data, it is necessary to analysis and check whether it is consistent or not. For this particular study, the consistency of recorded data for four stations checked by double mass curve and no need of corrections because they correlated. The result of a double mass curve for stations in the study watershed is shown in Figure 3.5, putting the cumulative of whole stations on the x-axis and cumulative of each station on the y-axis.

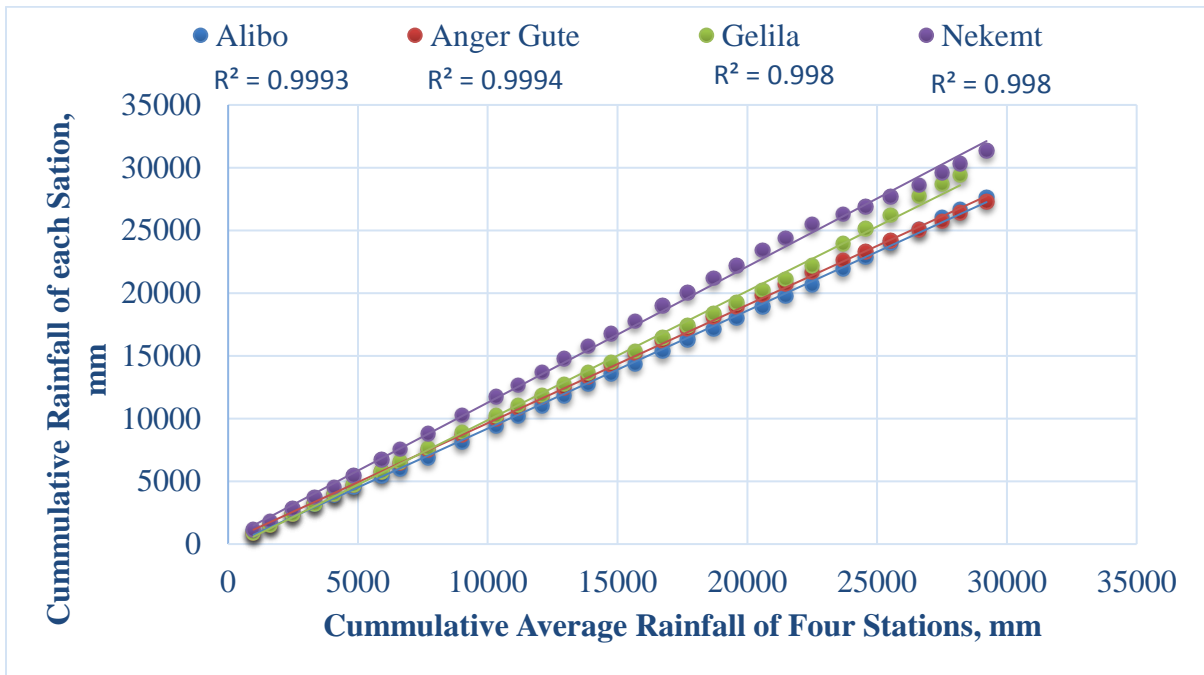


Figure 3.5 Double mass curve for stations in the watershed

### 3.3.2.3. Weather Generator

The three stations (Alibo, Anger Gute and Gelila) contain only precipitation and temperature (minimum and maximum) data. However, Nekemte station contains all climatic data such as precipitation, temperature (minimum and maximum), sunshine, relative humidity, and wind speed. Therefore, sunshine, relative humidity, and wind speed data generated for Alibo, Anger Gute and Gelila stations from Nekemte station. The parameters required for weather generator were calculated using software programs like; PCP STAT.exe and dew02.exe. The statistical parameters of daily precipitation data such as PCPMM, PCPSTD, PCPSKW, PR\_W1, PR\_W2, PCPD and RAINHHMX were calculated by the program PCP STAT.exe using daily precipitation. Whereas, the program dew02.exe calculated the average daily dewpoint temperature per month using daily air temperature and humidity data. The Calculated parameters for weather generator were adjusted and added into the SWAT weather database table.

### 3.3.2.4. Landsat image pre-processing

Bands of the similar spatial resolution were combined together through layer stacking. As one image could not cover the study area, two-layer stacked image was mosaicked for each year images. Because of their low spatial resolution 60m, 100m and 120m were not used for the analysis of land use land cover change. Since ETM+ and OLI\_TIRS have multispectral images of 30m and panchromatic image of 15m spatial resolution, image fusion (pan-sharpening) techniques were done to improve the visualization of images for better analysis of LULC. Clipping the mosaicked image with shapefile of the watershed was done by using ERDAS imagine 2015 through Subsetting to reduce the size of an image to the area of interest.

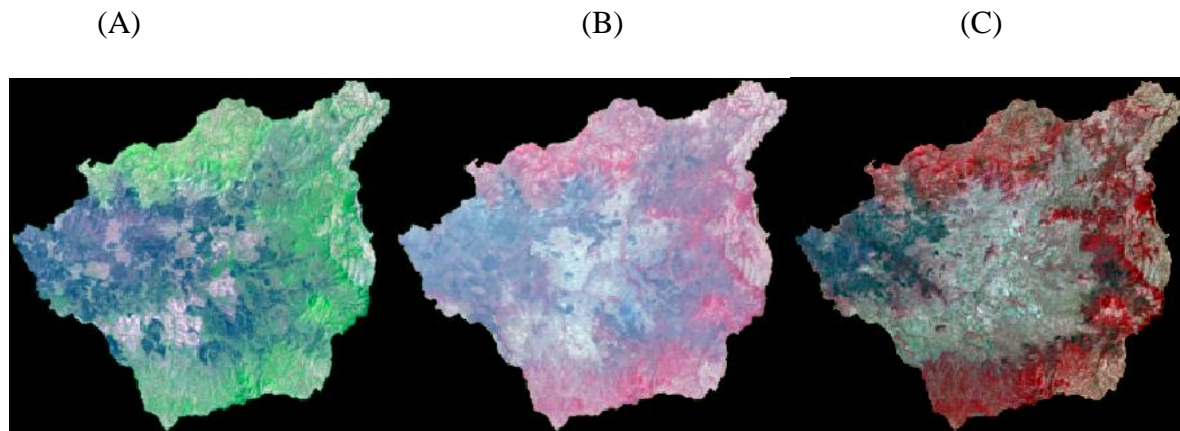


Figure 3.6 Subset images of (A) Landsat-5 (TM), (B) Landsat -7 (ETM+) and (C) Landsat- 8 (OLI\_TIRS)

### 3.3.2.5. Site observation

The site observation was done by two methods; moving through selected villages and looking for the present land use and land cover and interviewing people living a long time in the area about the land feature of the past. During the field observation, GPS was used for conducting land features at different coordinates for selected representative villages. The past land cover and their changes to other forms of land use were discussed with elders of the area. Both conducted data of the present and acquired information of the past was used for Landsat image classification and accuracy assessment.



### 3.3.3. Image classification

Image classification is the process of assigning defined land use land cover classes for pixels of a continuous raster image (Guide, 2010). There are unsupervised and supervised types of image classification systems. In Unsupervised classification method, the combined satellite images were classified by using an Iterative Self- Organizing Data Analysis Techniques algorithm (ISODATA) with ERDAS imagine software. ISODATA is a clustering algorithm that uses an iterative process to separate image pixels into spectrally similar clusters based upon their position in the dimensional spectral space (Enderle and Weih 2005). In this type of classification since it could not be supported with field work, one land feature might be classified as of another which will not much with ground truth.

However, in supervised classification pixels of similar spectral value could be classified into the same land use land cover classes based on ground truth of the area. For this study, the land classified with unsupervised classification was followed by supervised classification technique which was supported by field work for further definition of the classes and thematic map preparation by using ERDAS imagine (version 2015) software.

The Signature Editor in ERDAS imagine is an important tool for creating a supervised classification from selected areas of interest. Once each training area was developed on the image need to be classified, the spectral characteristics across all bands and all dates for each pixel in the training area were then inputted into the Signature Editor. The signature for that training area was labeled, evaluated, edited, merged for similar features and then incorporated into the supervised classification. The Signature Editor is a means of managing all of the spectral signatures from the training areas for the image(s) being classified (Enderle and Weih, 2005).

The supervised classification, using the maximum likelihood classification method, utilized 25 individual selected point in signature Editor for each selected year. Finally, for Hangar watershed six land use/land cover was identified and given the code having four letters which the SWAT model can understand as in Table 3.4. The SWAT codes given for six classes LULC of Hangar Watershed are; FRST (Forest-Mixed), RNGB (Range-Brush), PAST (Pasture), AGRL (Agricultural Land-Generic), URBN (Residential) and WATR (Water) for

Forest, Rangeland, Grassland, Cultivated land, Built-up area and Waterbody , respectively. The prepared maps were used independently to uncover the hydrological impacts of LULC changes in the study watershed.

Table 3.4 The classified land use/land cover of the study watershed with its SWAT code

Land use/ land cover type	Description	SWAT code
Water Body	Rivers, Streams	WATR
Range Land	Include areas covered with small trees, less dense forests and bushes and shrubs.	RNGB
Forest	Areas covered with dense growth of trees were included here.	FRST
Cultivated land and settlements	Include areas used for perennial and annual crops, irrigated areas and the scattered rural settlements.	AGRL
Grassland	Areas used for Livestock grazing, as well as bare land that has very little or no grass cover (exposed rocks) but with the same tone on the aerial photographs were included here.	PAST
Built-up Area	Areas used for construction sites, both zone and woreda's towns and also roads were classified here due to their similar reflectance.	URBN

#### 3.3.4. Accuracy assessment

The Land use/land cover map was prepared through supervised classification by utilizing the present land use and land cover data of the field collected by GPS, information of the past times from elders living at the study area and Google earth as a reference data. Finally, image classification accuracy was evaluated and summarized by the error matrix and kappa coefficients (Table 4.1, 4.2 and 4.3). Kappa value typically lies between 0 and 1 where, the value greater than 0.8 denotes a strong agreement and values between 0.75 and 0.8 are very good indicators of the classified image (Viera, and Garrett, 2005). The overall flowchart of the Landsat image pre-processing and classification is shown in figure 3.7.

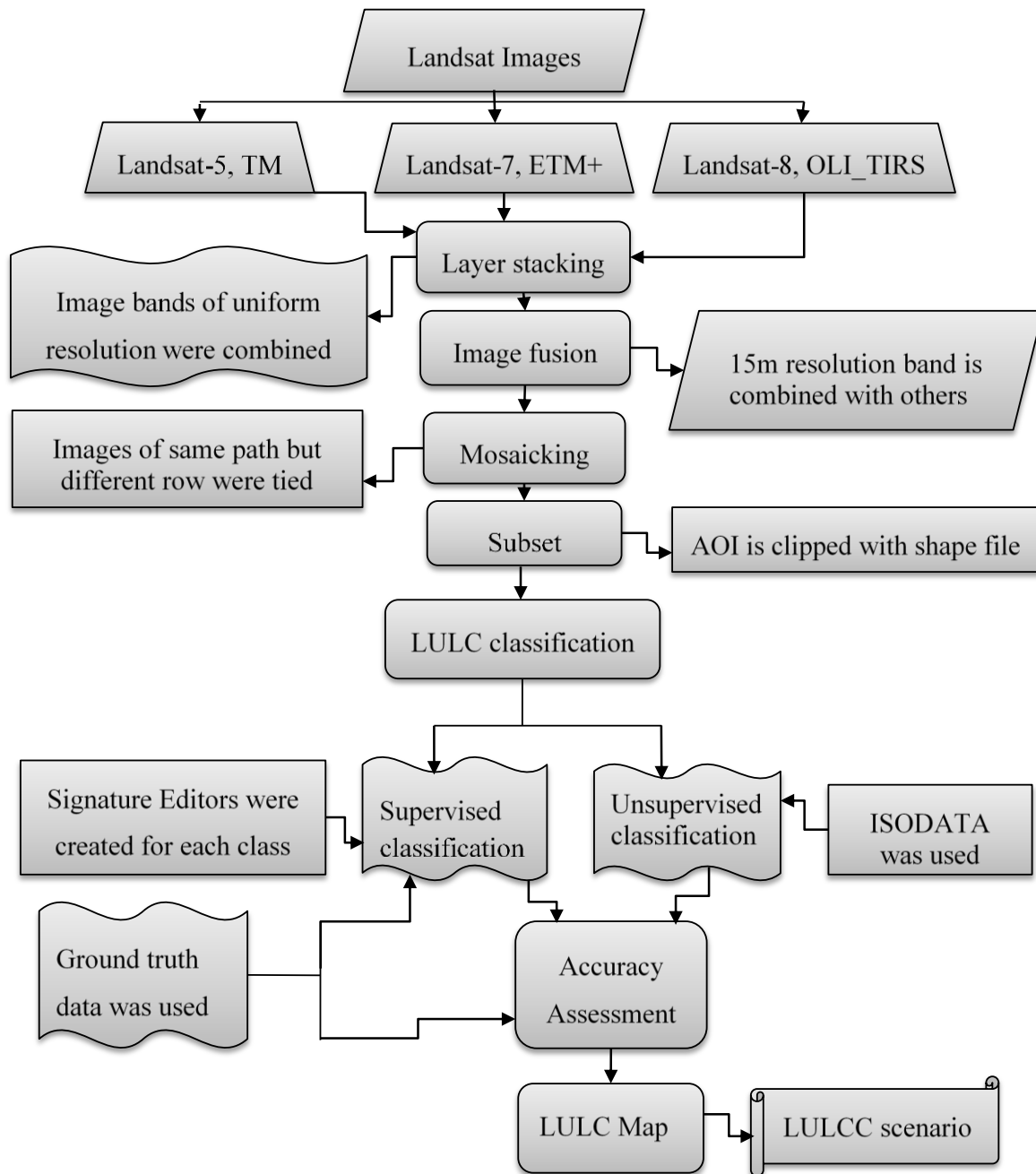


Figure 3.7 Flowchart of the Landsat image pre-processing and classification

### **3.4. Evaluation of the impacts of LULCCs on the hydrological process**

The dynamics of land cover and expansion and/or modification of land use could affect the hydrological processes of the watershed. Analyzing LULCC with a considerable attention enables to evaluate its effects on the hydrologic process. For this study, ERDAS imagine (2015) software in integration with the Arc SWAT (2012) model were used to analysis the modification and/or changes of land use/land cover and its impacts on hydrological processes of the Watershed. Hangar Watershed has experienced changes in land use/land cover from 1987 to 2017.

Three independent simulations for LULC of 1987, 2001 and 2017 were performed to examine the effects of this land use and land cover changes on the hydrological process. To evaluate the variability of hydrological process due to the land use/land cover changes, the SWAT model run using the three land use/land cover maps of 1987, 2001 and 2017 remaining the other inputs unchanged. The generated results of each year were imported into SWAT-CUP (Soil and Water Assessment tool-Calibration and Uncertainty Program). SUFI-2 (Sequential Uncertainty Fitting version two) algorithm linked to SWAT-CUP was used to calibrate and validate the model outputs using the observed streamflow data. After calibration and validation, the periodic variability of the hydrological process resulted from LULC changes were evaluated and compared interms of surface flow, ground water flow, sediment yield, evapotranspiration and water yield contributions to the streamflow.

### **3.5. Hydrological components of the SWAT model**

SWAT model is a physically based, semi-distributed parameter model with a robust hydrologic and pollution element that has been successfully employed in a number of watersheds (Winai *et al.*, 2013). Daily rainfall data, maximum and minimum air temperature, solar radiation, relative air humidity, and wind speed are the inputs used by this model and is able to describe water and sediment circulation, vegetation growth and nutrients circulation. SWAT was used to simulate the hydrologic processes of the study watershed. Simulations of the hydrology of a watershed can be separated into two major divisions. The first division is the land phase of the hydrologic cycle, and the second division is the water or routing phase of the cycle (Winai *et al.*, 2013) . In order to obtain accurate forecasting of water, nutrient and sediment circulation,

it is necessary to simulate hydrologic cycle which integrates overall water circulation in the catchment area. Hence the model uses the following water balance equation to simulate the land phase of the hydrological cycle in the catchment (Gayathri K Devi *et al.*, 2015).

$$SW_t = SW_0 + \sum_{i=1}^t (R_v - Q_s - W_{seepage} - ET - Q_{gw}) \quad [3.8]$$

Where  $SW_t$  is the final soil water content (mm water),  $SW_0$  is base/initial soil water content on day  $i$  (mm water),  $R_v$  is rainfall volume on day  $i$  (mm water),  $Q_s$  is the surface runoff on day  $i$  (mm water),  $W_{seepage}$  is the seepage of water from soil to underlying layers on day  $i$  (mm water),  $ET$  is the amount of evapotranspiration on day  $i$  (mm water),  $Q_{gw}$  is the amount of return flow on day  $i$  (mm water) and  $t$  is time in days.

### 3.5.1. The surface runoff Generation

The source of runoff is precipitation and it is generated when rainfall exceeds infiltration rate. The part of precipitation that is not intercepted by the plant canopy, not infiltrated into the soil, and not contributes for depression storage is excess rainfall and resulted in surface runoff generation. The SWAT model uses the SCS curve number procedure when daily precipitation data is used while the Green-Ampt infiltration method is chosen when sub-daily data is used to estimate surface runoff (Shen *et al.*, 2012). For this study, the SWAT used SCS curve number method to estimate surface runoff because the daily rainfall data is imputed into the model.

### 3.5.2. Evapotranspiration computation

Evaporation and transpiration occur simultaneously whereby water is lost on the one hand from the soil surface by evaporation and on the other hand from the crop by transpiration (Allen *et al.*, 1998). Potential Evapotranspiration (PET) is the rate at which evapotranspiration would occur from a large area uniformly covered with growing vegetation that has access to an unlimited supply of soil water and that was not exposed to heat storage effects. Numerous methods have been developed to estimate PET (Neitsch *et al.*, 2011). Three of this methods have been incorporated into the SWAT model: the Penman-Monteith method (Monteith, 1965) which requires solar radiation, air temperature, relative humidity and wind speed; the Priestley-Taylor method (Priestley and Taylor, 1972) that requires solar radiation, air

temperature and relative humidity and the Hargreaves method (Hargreaves et al., 1985) which needs air temperature to determine PET. Therefore, for this study, the SWAT model adopts Penman-Monteith method to estimate.

### 3.5.3. Groundwater

Groundwater is water in the saturated zone of earth materials under pressure greater than atmospheric. Water enters ground water storage by infiltration, although recharged by seepage from surface water bodies may occur. The SWAT model simulates two aquifers in each subbasin (Neitsch *et al.*, 2011). The shallow aquifer is an unconfined aquifer that contributes to flow in the main channel or reach of the subbasin. Water that enters the deep aquifer is assumed to contribute to the streamflow somewhere outside of the watershed.

### 3.5.4. Flow routing

For flow routing, the SWAT model uses Manning's equation to estimate the rate and velocity of flow (Wangpimool *et al.*, 2013). Water is routed through the channel network using the variable storage routing method or the Muskingum River routing method.

$$\Delta S = S_{in} - S_{out} \quad [3.9]$$

Where,  $\Delta S$  is the change in volume of storage during the time step ( $m^3$  water),  $S_{in}$  is the volume of inflow during time step ( $m^3$  water), and  $S_{out}$  is the volume of outflow during time step ( $m^3$  water).

## 3.6. The Model Set-Up

SWAT model was designed to predict the impact of land management practices on water, sediment and agricultural chemical yields in large complex watersheds with varying conditions over long periods of time (Arnold *et al.*, 2012). There are various producers with which SWAT model proceed to give output for which past procedure is an input for the next one. Looking for the next task without properly completing one of these steps is impossible.

### **3.6.1. SWAT project set up**

After completion of SWAT database preparation, the first procedures in the SWAT model is to create a new project or DEM set up of having identified folder in which the whole work could be executed.

### **3.6.2. Watershed delineation**

Watershed delineation is the division of basins into smaller sub-basins for determining their contributions to the main Stream. The watershed delineation interface in Arc SWAT is separated into five sections including DEM Set Up, DEM-based Stream Definition (flow direction and accumulation and drainage network generation), Outlet and Inlet Definition, Watershed Outlet(s) Selection and Definition and Calculation of Sub-basin parameters. In order to delineate sub-basins networks, a critical threshold value is required to define the minimum drainage area required to form the origin of a stream. After the initial sub-basin delineation, the generated stream network can be edited and refined by the inclusion of additional sub-basin inlet or outlets. Adding an outlet at the location of established monitoring stations is useful for the comparison of flow concentrations between the predicted and observed data. Therefore, one basin outlet was manually edited into the watershed based on the known stream gage location that had streamflow data. As Vilaysane *et al.*, (2015) indicated, the smaller the threshold area, the more detailed the drainage networks and the number of sub-basins and HRUs. In this study, the smaller area (7600 ha) is provided to get 61 sub-basins of the Hangar river basin and outlet is defined, in which it is later taken as a point of calibration of the simulated flows. The delineated catchment is shown in figure 3.8.

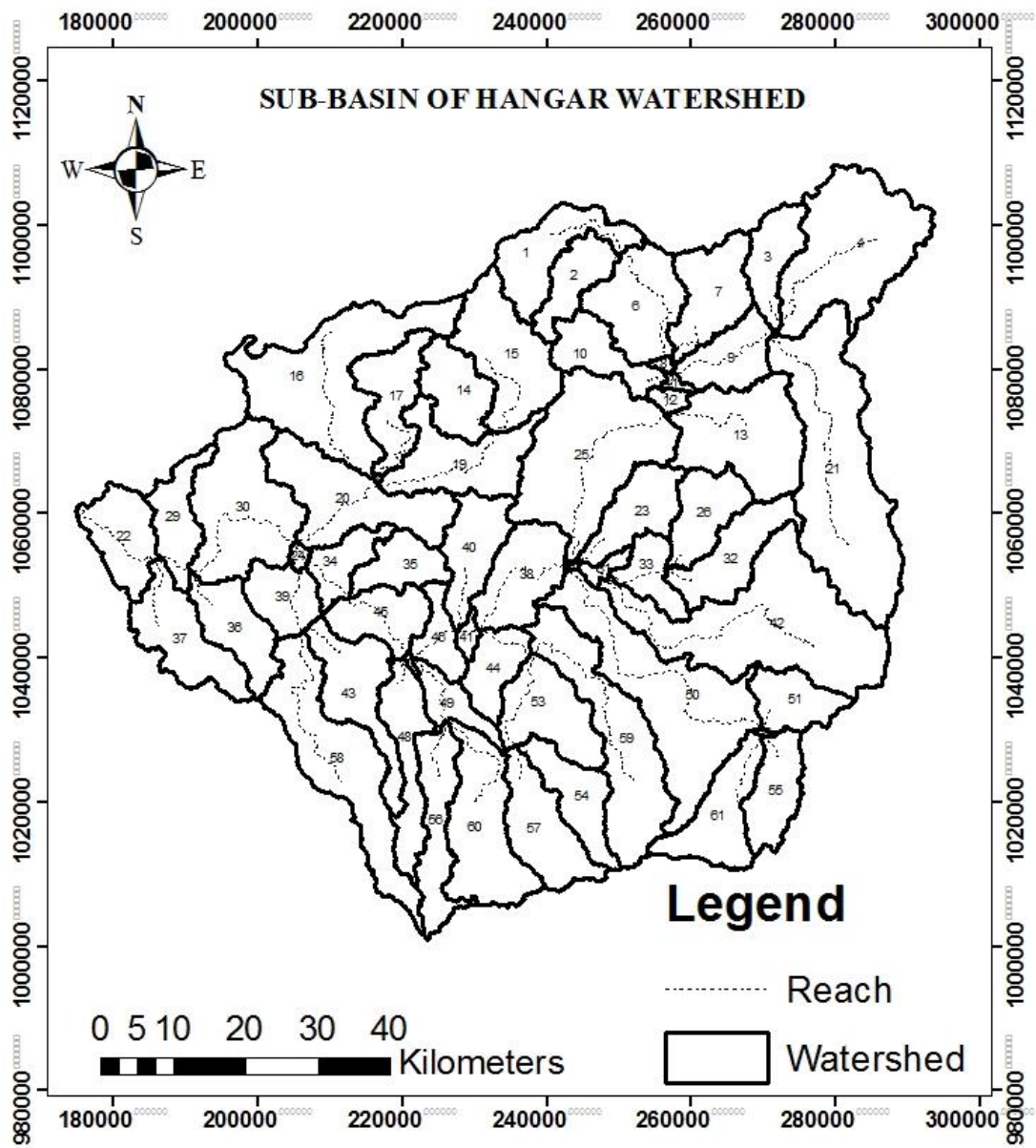


Figure 3.8 Hangar Watershed

### 3.6.3. HRUs analysis

SWAT model used spatial data such as land use, soil, and slope to create different Hydrologic Response Units (HRUs) analysis system, which are the unique combinations of land use soil and slope type within each sub-basin. The multiple scenarios that account for 15% land use, 15% soil and 15% slope threshold combination give a better estimation of stream flow. As the percentage of land use, slope and soil threshold increases, the actual evapotranspiration



decreases due to eliminated land use classes (Vilaysane *et al.*, 2015). Taking objective of the study into consideration and paying attention to characteristics of HRUs as the key factors affecting the stream flow, a land use, soil and slope class threshold of 10%, 15%, and 15% were used respectively. Hence, the Hangar River basin results in 196 HRUs in the whole basin. Categorizing sub-basins into HRUs increases accuracy and provides a much better physical description (Mtaló *et al.*, 2012). The SWAT model predicts the impacts at the subbasin (sub-watershed) or further at the Hydrologic Response Units (HRUs) (Gashaw *et al.*, 2018 and Arnold *et al.*, 2012). The land use and soil classifications for the model are slightly different than those used in many readily available datasets and therefore the land use and soil data were reclassified into SWAT land use and soil classes prior to running the simulation. Definition and reclassification of Land use dataset, the definition of soil dataset, reclassification of soil and slope layers and overlay of land use, soil and slope layer were done during Hydrologic Response Unit analysis. The prepared soil layers classified LULC and slope layers and delineated Watershed by Arc SWAT were overlapped 100%. The reclassified SWAT land use/land cover, soil and slope are shown in Figure 3.9.

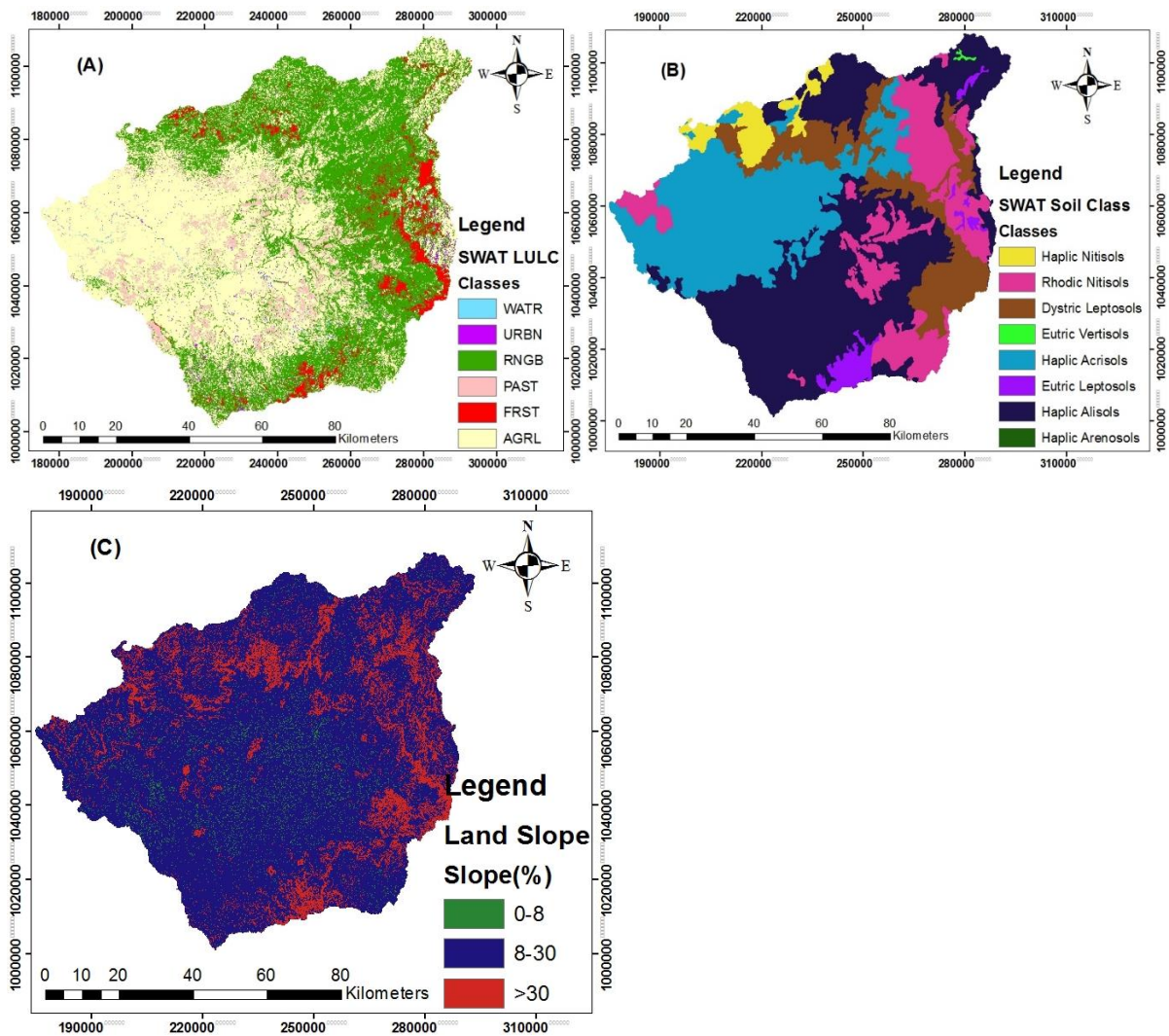


Figure 3.9 The SWAT LULC (A), Soil (B) and Slope (C) classes of Hangar Watershed

Table 3.5 Slope classes and its area of coverage

Slope Classes	Range	Area of coverage	
		(ha)	(%)
Class 1	0-8	852.65	11.11
Class 2	8-30	1705.31	22.22
Class 3	>30	5115.91	66.67
Total		7673.87	100

#### **3.6.4. Write input tables**

Spatial scale data such as land use/land cover, soil and slope were defined and analyzed in Hydrologic Response Units analysis (HRUs). The time scale data such as Rainfall data, Temperature data, Relative Humidity data, Solar Radiation data, and Wind speed data were prepared in the text format. The Weather generator data was developed for the principal station and imported into the SWAT database to generate solar radiation data, wind speed data and relative humidity data for secondary stations. The prepared time scale data and the developed weather generator data were loaded and written in this stage of model setup.

#### **3.6.5. Edit SWAT input**

The modification of the SWAT model database and input files is allowed in the edit SWAT input. The incorrectly inputted data could be edited so that correct output would be generated.

#### **3.6.6. SWAT simulation**

The input to the model is finalized and the output is generated and read after running the model in the SWAT simulation. For this study, the SWAT model was run with the historic meteorological data of 1987 to 2017 by keeping three years (1987-1989) for warm-up period to avoid the impacts of the initial conditions of the model.

### **3.7. The SWAT-CUP Model**

The output files, which could obtained after the SWAT model run are the results, generated corresponding to measured data and need to be calibrated and validated. SWAT-CUP is an interface developed to provide a link between the input/output of a calibration program and the SWAT model (User Manual, 2014). It is a program used to implement parallel processing (SWAT Calibration and Uncertainty Procedures) (Rouholahnejad, 2012). After the model run, the SWAT-CUP requires outputs, which extracted from the model output files to do automate calibration. The uncertain model parameters are selected roughly at the beginning and systematically changed looking at their sensitivity after each simulation. Finally, the most sensitive parameters with which the hydrology of the watershed could influenced are identified and the model calibration and validation were performed by SWAT-CUP through SUFI-2.

### **3.7.1. Parameter Sensitivity analysis**

Sensitivity analysis is the process of determining the rate of change in model output with respect to changes in model inputs (parameters) (Moriassi *et al.*, 2007). It is a necessary process to identify key parameters and parameter precision required for calibration and validation of the SWAT model. For this study, to identify the most important SWAT parameters, at the beginning 18 flow parameters (Appendix B) were selected from SWAT-CUP (Absolute\_SWAT\_Value.txt). In the SWAT-CUP sensitivity analysis of parameters can be performed in two ways: Global sensitivity analysis which allows changing each parameter at a time and One-at-a-time sensitivity analysis which performs one parameter at a time only (Arnold *et al.*, 2012). For this purpose, global sensitivity analysis was employed in SWAT-CUP 2012. ). The measure and significance of sensitivity were provided by indices such as t-stat and p-value, respectively (Chaibou Begou *et al.*, 2016; Abbaspour, 2013) where, higher t-test in absolute values measures high sensitivity and zero p-value represents more significant.

### **3.7.2. Uncertainty Analysis**

As Yang *et al.*, 2008 suggested, uncertainties in distributed models may arise from model input uncertainty, conceptual model (structural uncertainty), parameter uncertainty and response uncertainty. To get a good result and support decisions about alternative management strategies in the areas of land use and land cover change, climate change, water allocation, and pollution control, it is important that the model pass through a careful calibration and uncertainty analysis. For this study uncertainty analysis was carried out through SUFI-2 algorithm which performed parameter uncertainty accounted for all uncertainty.

### **3.7.3. Model calibration and validation**

The Calibration is the tuning or adjustment of model parameters and their values, within the recommended ranges, to optimize the model output so that it matches with the measured set of data (Vilaysane *et al.*, 2015). These parameters could be adjusted manually or new parameters of past iteration would be copied from New\_pars.txt to par\_inf.txt for the continued iteration until the model output best matches with the observed data. This involves comparing the model results, generated with the use of historic meteorological data, to recorded stream flows. This

study used Sequential Uncertainty Fitting-2 (SUFI-2) algorithm in SWAT-CUP 2012 for calibrating model outputs using gauged stream flow. The validation is the process of determining the degree in which a model or simulation is an accurate representation of the observed set of data from the perspective of the intended uses of the model (Abraham *et al.*, 2007). It is a comparison of the model outputs with an independent dataset without further adjustments of the values of the parameters (Abraham *et al.*, 2007). The process continued until the simulation of validation period of the stream flows confirmed that the model performs satisfactorily. Therefore, in this study, calibration and validation were carried out using 25 years (1987–2011) of daily-observed flow data. The data was divided into model warm-up (1987-1989), calibration (1990–2002) and validation (2003–2011) periods. For a better parameterization of the SWAT model and to reduce the model output uncertainty (Gashaw *et al.*, 2018), a longer calibration period was used.

#### **3.7.4. The model performance evaluation**

Standard regression statistics like coefficient of determination ( $R^2$ ) and Nash-Sutcliffe efficiency (NSE) determine the strength of the linear relationship between simulated and measured data (Moriasi *et al.*, 2007).  $R^2$  ranges from zero to one, with higher values indicating less error variance, and typically values greater than 0.5 are considered acceptable (Santhi *et al.*, 2001; Van Liew *et al.*, 2007).

NSE ranges between  $-\infty$  and one, with  $NSE = 1$  being the optimal value. Values between zero and one are generally viewed as acceptable levels of performance, whereas values less than zero indicates that the mean observed value is a better predictor than the simulated value, which shows unacceptable performance (Moriasi *et al.*, 2007). Percent bias (PBIAS) measures the average tendency of the simulated data to be larger or smaller than their observed counterparts in which the optimal value of PBIAS is 0.0, with low-magnitude values indicating accurate model simulation (Gupta *et al.*, 1999). The SWAT model evaluation guideline based on performance rating was given in Table 3.7. Hence, for this study, the performance of the SWAT model was checked using values of  $R^2$ , NSE and PBIAS based on their performance rating (Table 3.7). Details of the methodology followed in this study are shown in Figure 3.11.

Table 3.6 The reported performance ratings for  $R^2$ , NSE and PBIAS for SWAT model

Modeling Phase	$R^2$	NSE	PBIAS	Performance rating
Calibration and Validation	$0.75 < R^2 \leq 1.00$	$0.75 < NSE \leq 1.00$	$PBIAS \leq \pm 10$	Very good
Calibration and Validation	$0.65 < R^2 \leq 0.75$	$0.65 < NSE \leq 0.75$	$\pm 10 \leq PBIAS \leq \pm 15$	Good
Calibration and Validation	$0.50 < R^2 \leq 0.65$	$0.50 < NSE \leq 0.65$	$\pm 15 \leq PBIAS \leq \pm 25$	Satisfactory

Source: Vanliew *et al.*, 2003

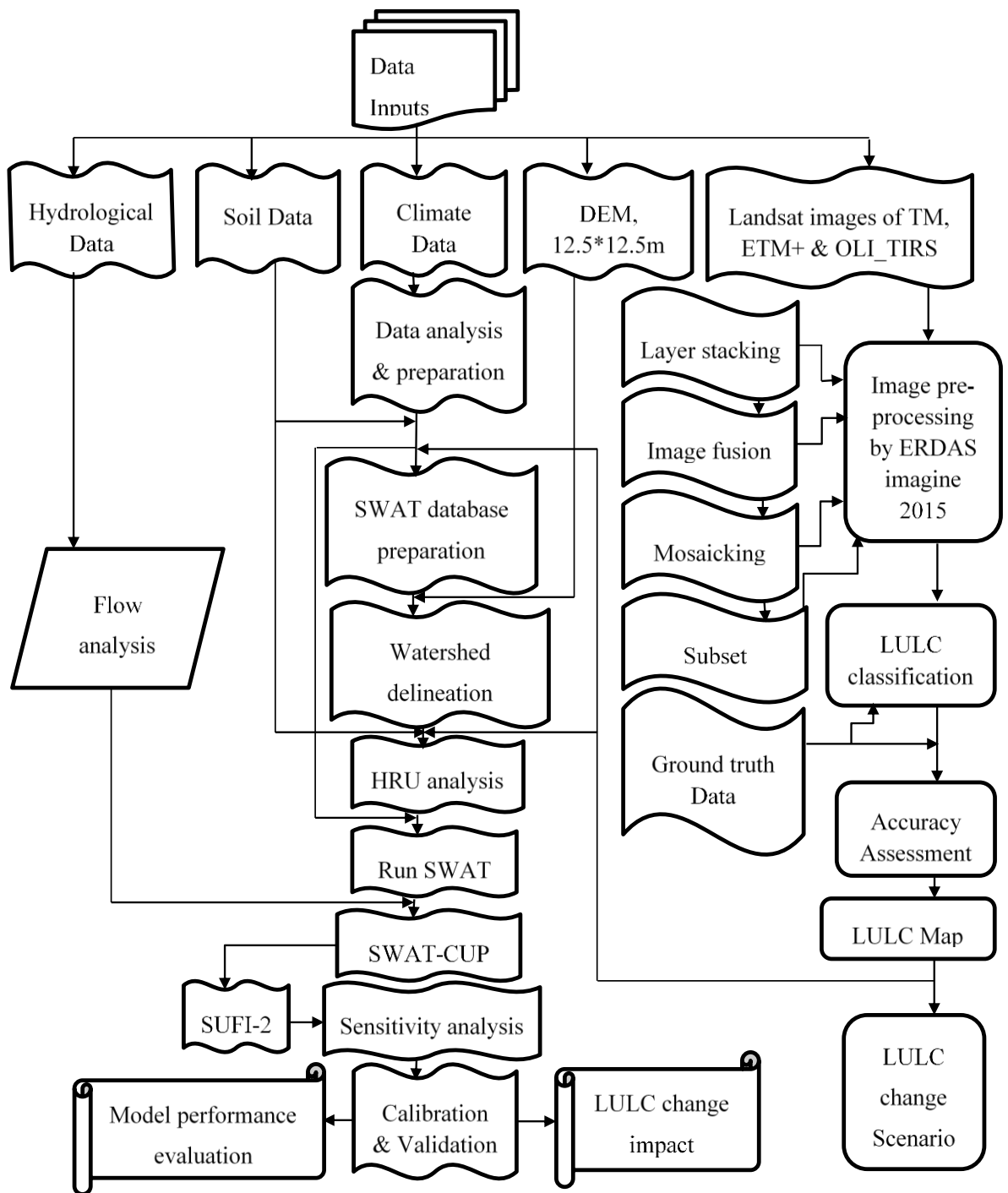


Figure 3.10 Flow chart of the research approach

## 4. Results and Discussion

### 4.1. Land use/land cover change assessment

#### 4.1.1. Land use/land cover Classification accuracy assessment

The overall accuracy of the classification was 84.38%, 87.78% and 86.90% for the period 1987, 2001 and 2017 respectively. A Kappa coefficient of above 0.80 was also obtained for the three classified images. Therefore, the validation data set indicated a very good agreement of the classified image with the ground truths. The accuracy report of the three classified images are shown in (Table 4.1, 4.2 and 4.3).

Table 4.1 Accuracy assessment of classified LULC of Hangar watershed in 1987

1987	Reference data									
Classified image (22-Jan-1987)		RNGB	PAST	CULT	FRST	URBN	WATR	Row total	User's accuracy (%)	Kappa coefficient
	RNGB	16	0	0	0	0	0	16	100	1
	PAST	0	12	1	2	1	0	16	75	0.7073
	CULT	1	0	13	1	0	1	16	81.25	0.7805
	FRST	1	1	0	14	0	0	16	87.5	0.84
	URBN	0	1	0	3	11	1	16	68.75	0.6471
	WATR	0	0	0	1	0	15	16	93.75	0.9241
	Column total	18	14	14	21	11	17	96		
Producer's accuracy (%)	88.89	85.71	92.86	66.7	100	88.24		Overall classification accuracy = 84.38 %	Overall kappa statistics = 0.8129	

Table 4.2 Accuracy assessment of classified LULC of Hangar watershed in 2001

2001	Reference data									
Classified image (05-Feb-2001)		RNGB	PAST	CULT	FRST	URBN	WATR	Row total	User's accuracy (%)	Kappa coefficient
	RNGB	15	0	0	0	0	0	15	100	1
	PAST	0	14	1	0	0	0	15	93.33	0.9167
	CULT	1	0	13	0	1	0	15	86.67	0.8442
	FRST	0	0	0	14	1	0	15	93.33	0.92
	URBN	0	3	0	1	11	0	15	80	0.7692
	WATR	1	1	0	0	1	12	15	73.33	0.68
	Column	17	18	14	15	15	12	90		
Producer's accuracy (%)	88.24	77.8	100	93.33	100	73.33		Overall classification accuracy = 87.78 %	Overall kappa statistics = 0.8533	



Table 4.3 Accuracy assessment of classified LULC of Hangar watershed in 2017

2017	Reference data									
Classified image (08-Jan-2017)		RNGB	PAST	CULT	FRST	URBN	WATR	Row total	User's accuracy (%)	Kappa coefficient
	RNGB	11	0	1	0	0	2	14	78.57	0.75
	PAST	0	12	0	1	1	0	14	85.71	0.831
	CULT	1	1	10	1	1	0	14	71.43	0.6712
	FRST	0	0	0	13	1	0	14	92.86	0.9104
	URBN	0	0	0	0	14	0	14	100	1
	WATR	0	0	0	1	0	13	14	92.86	0.9155
	Column total	12	13	11	17	17	13	84		
	Producer's accuracy (%)	91.67	92.31	90.91	76.47	82.35	100		Overall classification accuracy = 86.90 %	Overall kappa statistics = 0.8432

#### 4.1.2. Land use/land cover change

During 1987–2017, significant amount of LULC changes occurred in the watershed. For example, cultivated land increased from 48.8% in 1987, to 64.0% in 2001, to 68.0% in 2017 periods. Correspondingly, the extent of built-up area was increased between 1987 and 2001 periods (1.3 to 1.7%), and the increment continued in 2017 (2.1%). Conversely, areas covered by forest decreased from 5.0% in 1987 to 4.0% in 2001, to 3.4% in 2017. Similarly, the extent of Range Land, grasslands and Waterbody were reduced throughout 1987, 2001 and 2017 periods (Figure 4.1).

Table 4.4 Summary of areas of LULC of Hangar Watershed through 1987 to 2017

LULC categories	1987		2001		2017	
	Area (ha)	Area (%)	Area (ha)	Area (%)	Area (ha)	Area (%)
Cultivated Land	374506.3	48.8	490832.3	64.0	521895.0	68.0
Rangeland	300338.4	39.1	216036.3	28.2	188712.4	24.6
Forest	38087.6	5.0	30331.9	4.0	25741.1	3.4
Grassland	41791.7	5.4	14688.5	1.9	13793.8	1.8
Built-up area	10088.9	1.3	12972.9	1.7	16077.8	2.1
Water Body	2574.0	0.3	2525.3	0.3	1167.1	0.2
Total	767387	100	767387	100	767387	100

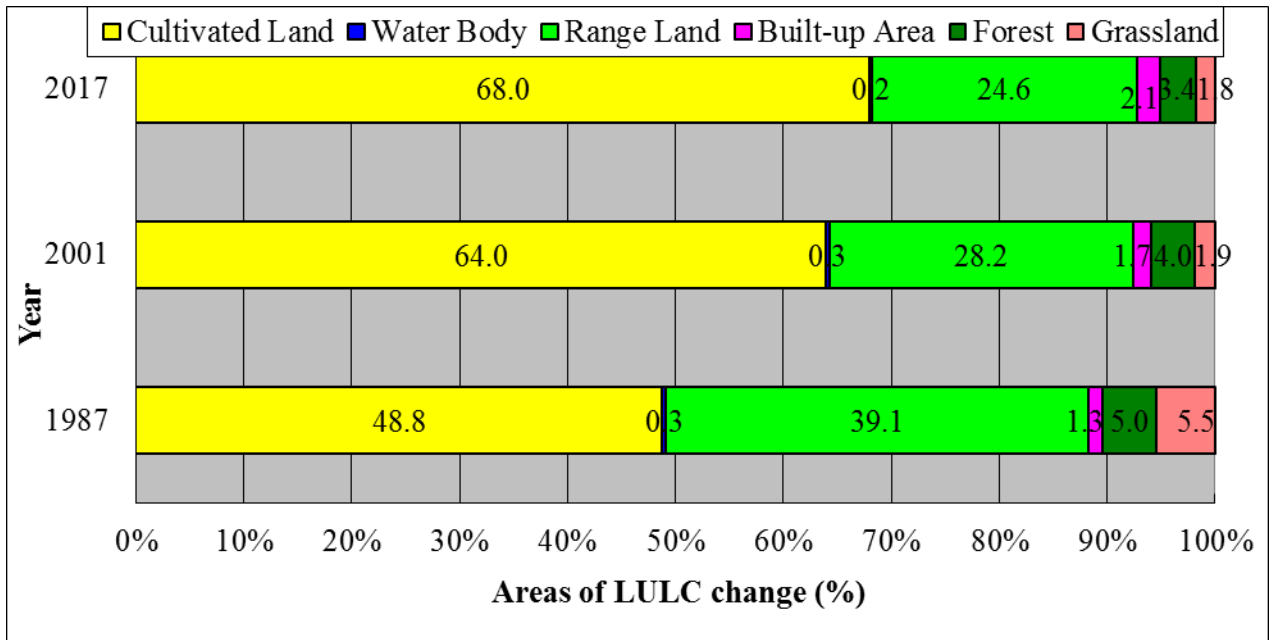


Figure 4.1 Areas of land use /land cover change in 1987, 2001 and 2017

#### 4.1.3. Land use/land cover Maps

The Landsat images of the Watershed area were pre-processed and classified using ground truth data. The maps of Classified LULC were prepared by using Arc map. The LULC states of the Hangar watershed through 1987 to 2017 periods are shown in Figure 4.2.

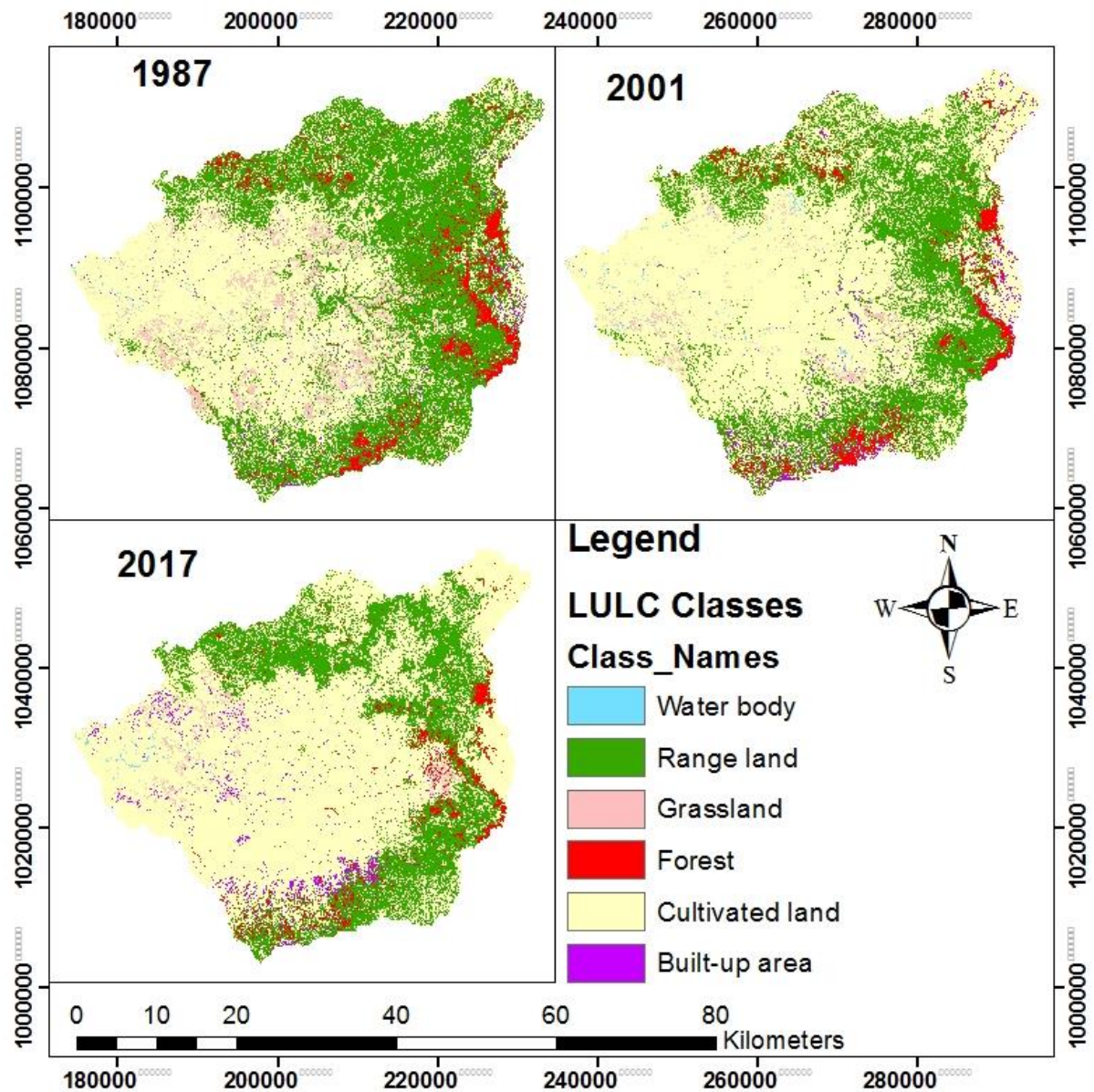


Figure 4.2 Land use/land cover map of the study area in 1987, 2001 and 2017

#### 4.1.4. LULC change analysis between 1987-2001, 2001-2017 and 1987-2017

The rapid increment of the built-up area during 1987–2001, 2001–2017 and 1987-2017 periods were observed because of residential woreda towns are expanded and to some extent of Nekemt town, the capital city of East Wollega Zone. Agricultural development was also consistent with this trend. For the study periods, however, the annual expansion rate (ha/yr) of Cultivated land until 2017 is greater than the built-up area (Table 4.5). Contrarily, forest, rangeland, grassland,

and Waterbody experienced a reduction in converge throughout the study periods. However, the greatest reduction rate (ha/yr) was observed in grassland (Table 4.5), which indicates that the expansion of cultivated land is utmost from grassland. Population growth and reduction of land productivity are expected to be the drivers of Waterbody reduction and built-up area expansion. The finding of this study is consistent with other studies carried out by Tekle, and Hedlund, 2000 in Kalu District and Gashaw *et al.*, 2018, where cultivated land increased at the expense of a reduction in forest and rangeland. The expansion of cultivated land and the shrinkage of forest were also reported by Zeleke, and Hurni, 2001 in Northern Ethiopian highlands; Bewket and Sterk, 2004 in Chemoga watershed and Garedew *et al.*, 2009 in the Central Rift Valley of Ethiopia. The increase of built-up area in this study watershed also coincides with other research findings in Ethiopia such as, Gashaw *et al.*, 2018 in the Andassa watershed; Belay 2002 in Derekolli catchment and Girmay 2003 in South Wello. The rate with which land use and land cover changed is larger in between 1987-2001 than in between 2001-2017. The idea gained from elders living in the study area also showed similar phenomena. Before 1991 the center of the watershed was known by the state farm which covered small area. Beginning from 1991 after the fall of Dergue regime in addition to state farm land protected area was occupied by tillers. Around 1992-2000 forest was cleared highly and agricultural land expanded. Beginning 2001 the land was unproductive due to highly plough that enforced land owners to leave such area free of till. The area left free of plough begun to cover by natural grass and some farmer plant tree on it. However since the top soil is removed by erosion its ability to take water in to it in the form of infiltration is reduced.

Table 4.5 Analysis of LULC change between 1987-2001, 2001-2017 and 1987-2017

LULC categories	1987	2001	2017	1987-2001		2001-2017		1987-2017	
	Coverage	Coverage	Coverage	Rate of change		Rate of change		Rate of change	
	Area (ha)	Area (ha)	Area (ha)	%	Ha/yr	%	Ha/yr	%	Ha/yr
Cultivated Land	374506	490832	521895	23.7	8309	6	19441	28.2	4913
Rangeland	300338	216036	188712	-28.1	-6021.6	-12.6	-1708	-37	-3721
Forest	38087.6	30331.9	25741.1	-20.4	-554	-15.1	-286.9	-32	-411.6
Grassland	41791.7	14688.5	13793.8	-64.9	-1935.9	-6.1	-55.9	-67	-933.3
Built-up area	10088.9	12972.9	16077.8	22.2	206	19.3	194.1	37.2	199.6
Water Body	2574	2525.3	1167.1	-1.9	-3.5	-53.8	-84.9	-55	-46.9
Total	767387	767387	767387						

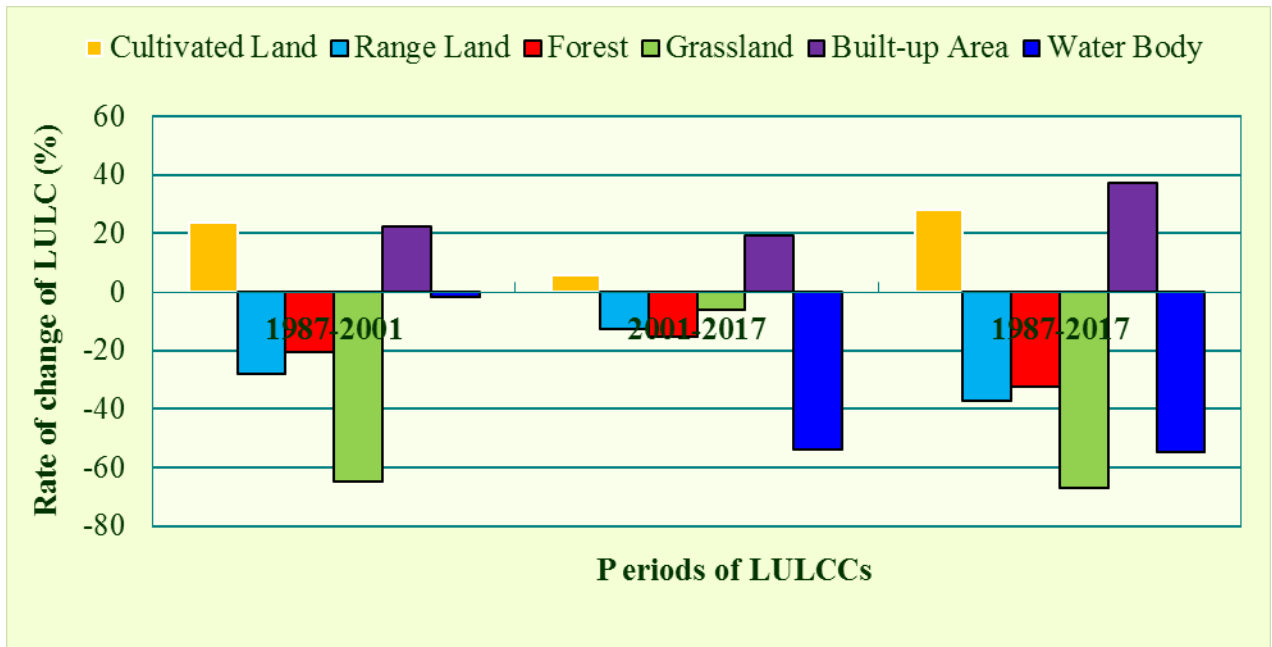


Figure 4.3 The analysis of Land use/land cover changes through 1987 to 2017

#### 4.2. Sensitivity analysis

The SWAT model generated an output which was processed using land use land cover, soil, and slope as an input. The model output needs analysis under the changed parameter, after which hydrological impacts of LULCC could be discussed. The sensitivity of output of the SWAT model to changes in parameter was studied under sensitivity analysis. Parameter sensitivity analysis helps focus the calibration and uncertainty analysis and is used to provide statistics for goodness-of-fit (Arnold *et al.*, 2012).

Because of the involvement of a wide range of data and parameters in the simulation process, calibration of outputs of big hydrological models like SWAT was quite a bulky task (Shimelash *et al.*, 2018). Hence, sensitivity analysis minimizes the number of parameters to be used in the calibration and/or validation iteration and shorten the time required for it by identifying the most sensitive parameters largely controlling the behavior of the simulated process (Zeray *et al.*, 2006). Sensitive parameters are selected randomly at the beginning of calibration and modified looking at their degree of sensitivity in SWAT-CUP SUFI2 from Global sensitivity at the end of each iteration. The sensitivity analysis, which was carried out using 18 SWAT parameters, identified the 13 most sensitive parameters controlling the output variable and with

which goodness-of-fit was reached. The 13 most sensitive parameters are ranked based on its t-stat and p-value (Table 4.6).

Table 4.6 The most sensitive parameters with its rank of sensitivity

No	Parameter Name	t-Stat	p-value	Rank of sensitivity
1	r__CANMX.hru	1.63	0.13	3
2	r__REVAPMN.gw	0.58	0.57	10
3	r__SOL_ALB().sol	0.01	0.99	13
4	r__CN2.mgt	-4.53	0	1
5	v__ALPHA_BF.gw	0.94	0.37	7
6	v__GW_DELAY.gw	1.31	0.22	4
7	v__GWQMN.gw	-0.82	0.43	8
8	r__GW_REVAP.gw	-0.97	0.35	6
9	r__ESCO.hru	-0.2	0.85	12
10	r__ALPHA_BNK.rte	0.7	0.5	9
11	r__SOL_AWC().sol	0.46	0.65	11
12	r__SURLAG.bsn	-2.02	0.07	2
13	r__EPCO.hru	-1.23	0.24	5

### 4.3. Flow Calibration using SUFI-2 Algorithm

The model generated output using model input parameters which kept within a realistic uncertainty range (Arnold *et al.*, 2012). Therefore, to have the physical knowledge of the watershed, calibration carried out using SWAT-CUP (SWAT-Calibration and Uncertainty Programs) through Sequential Uncertainty Fitting-2 (SUFI-2). The SWAT model output was calibrated using 13 years measured streamflow data (1990-2002). The obtained  $R^2$  and NSE value during calibration were 0.87 and 0.82 respectively. The graphical comparison of observed and simulated flow during calibration are shown in Figure 4.4, 4.5, 4.6, 4.7, 4.8 and 4.9 for the corresponding years of study.

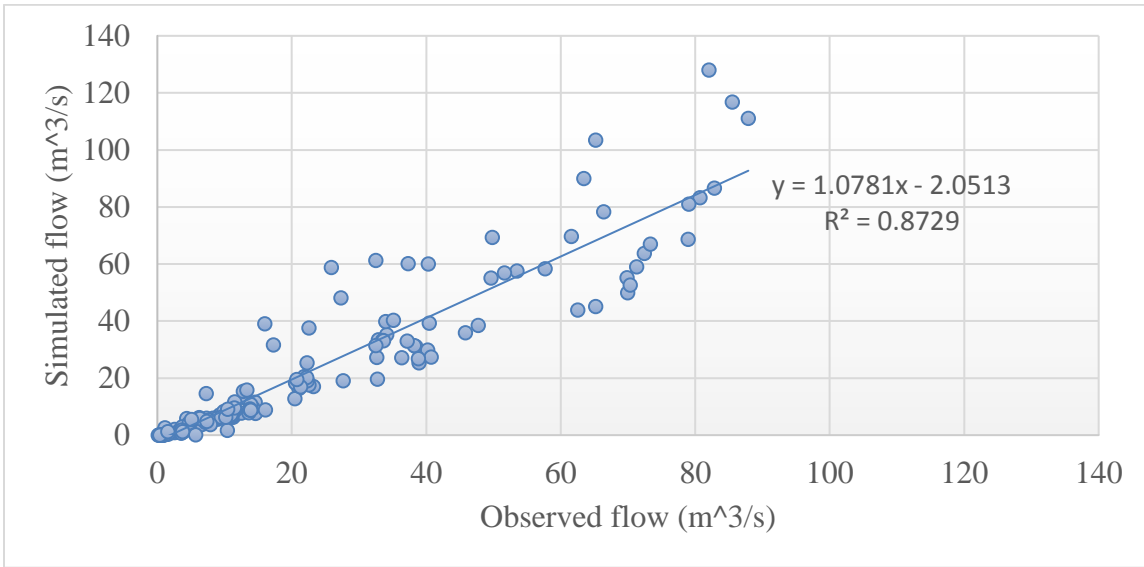


Figure 4.4 Graph of simulated versus observed flow during calibration for LULC of 1987

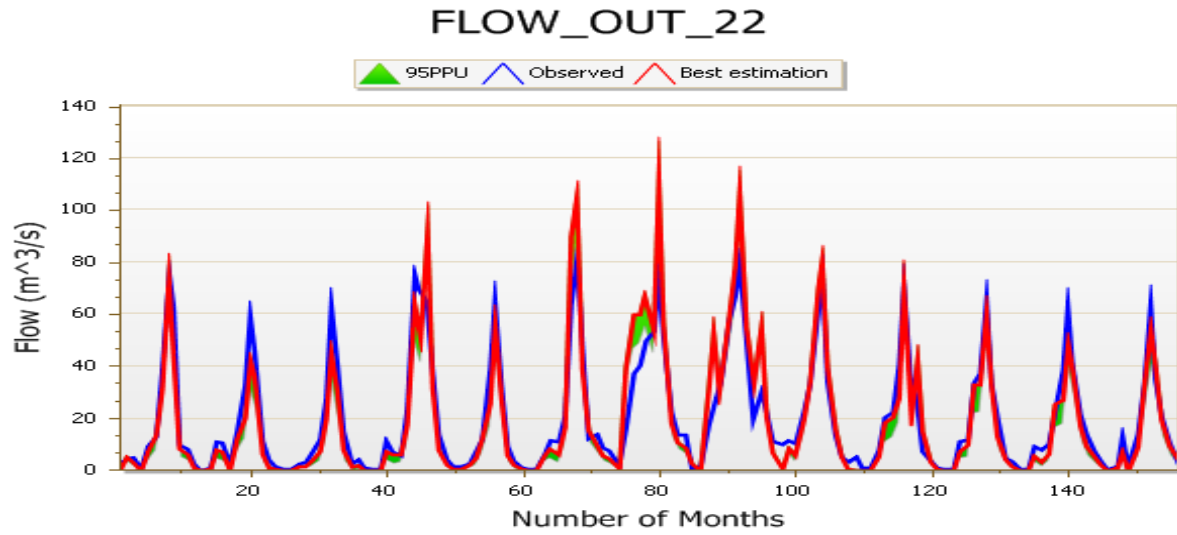


Figure 4.5 Hydrograph of Monthly simulated and observed flow during calibration for LULC of 1987

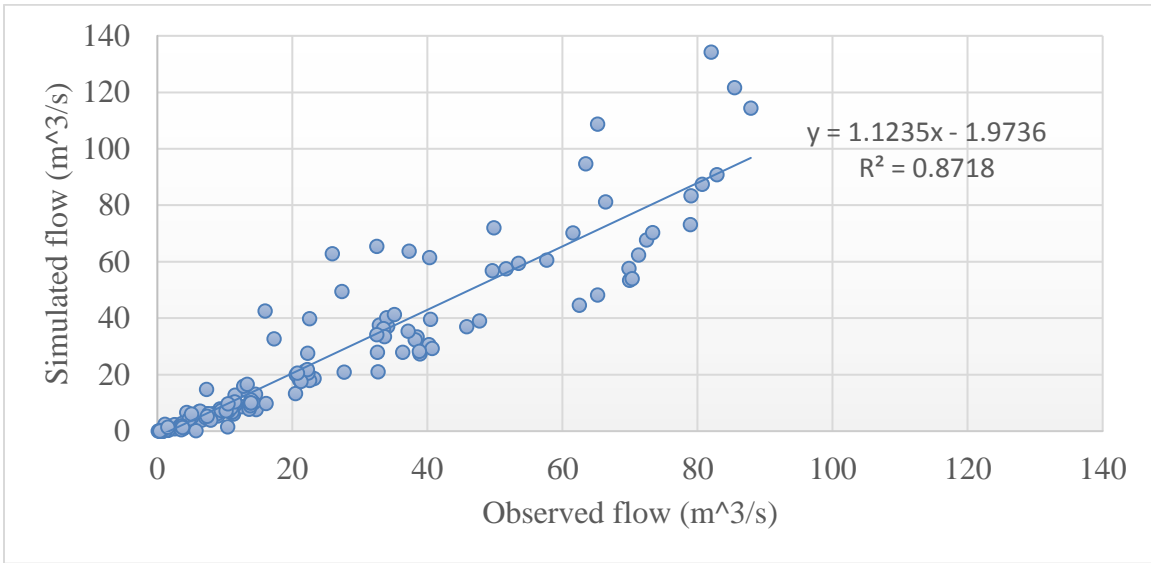


Figure 4.6 Graph of simulated versus observed flow during calibration for LULC of 2001

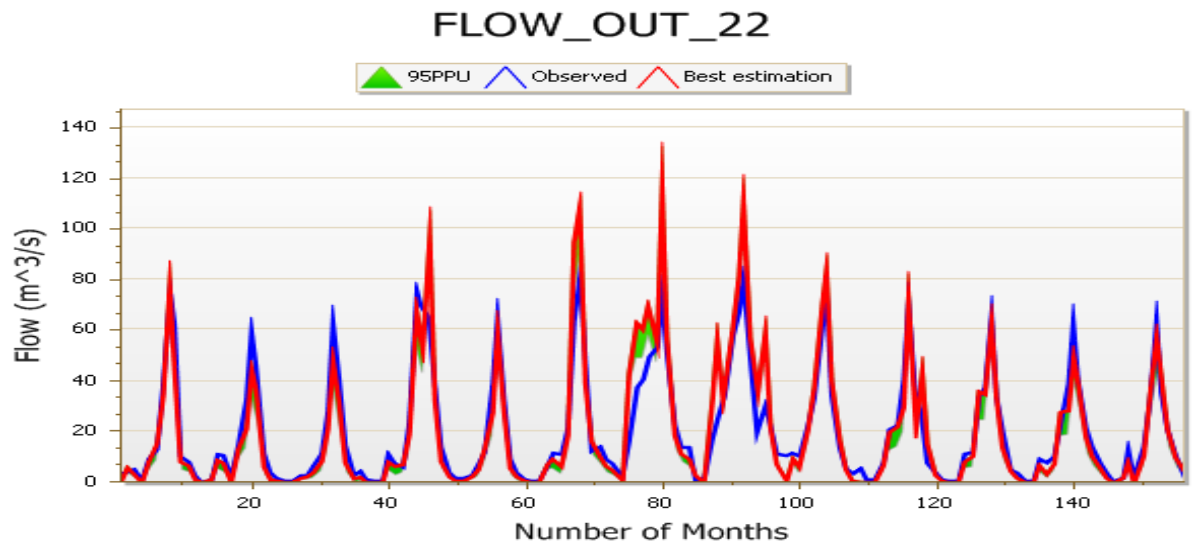


Figure 4.7 Hydrograph of Monthly simulated and observed flow during calibration for LULC of 2001



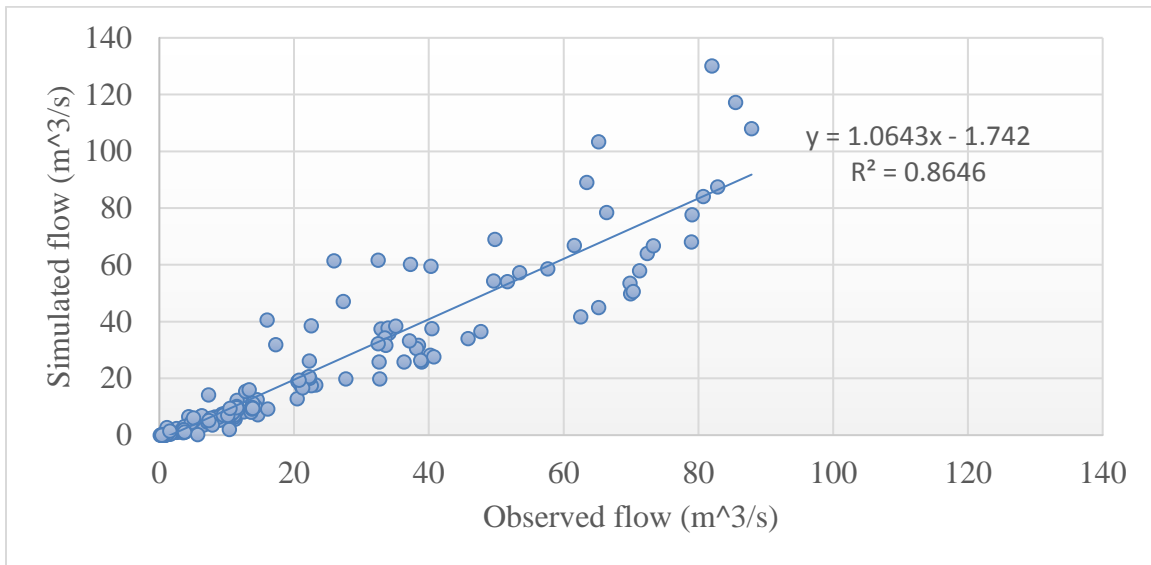


Figure 4.8 Graph of simulated versus observed flow during calibration for LULC of 2017

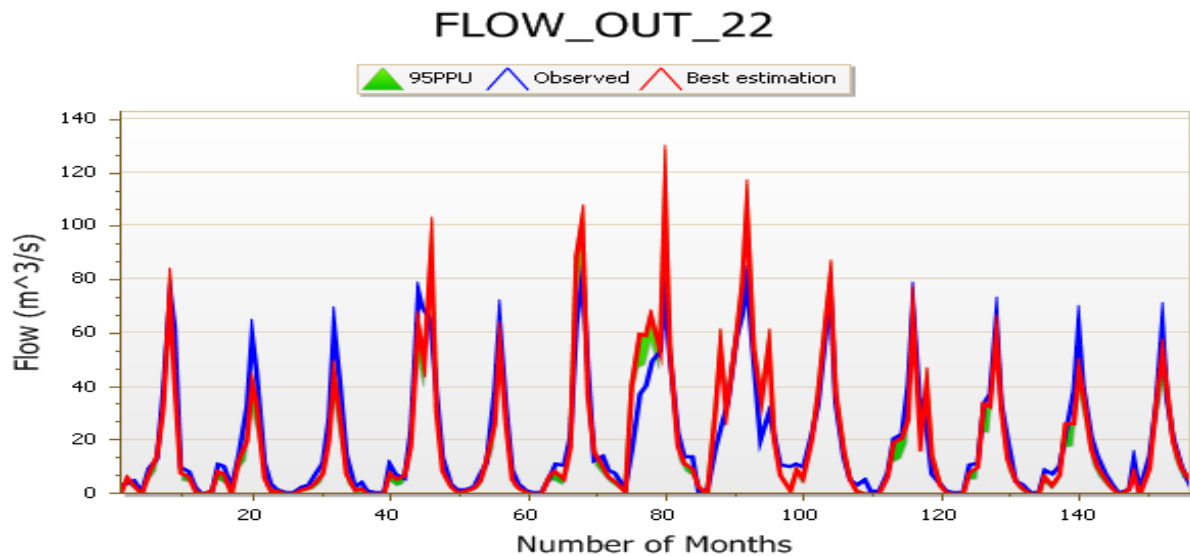


Figure 4.9 Hydrograph of Monthly simulated and observed flow during calibration for LULC of 2017

#### 4.4. Flow Validation using SUFI-2 algorithm

For the catchment with longtime series split sample test is involved (Shimelash M. et al., 2018) for which one part is used to calibrate the model, and the second part is used for testing (validating) if calibrated parameters produced simulations which satisfy goodness-of-fit tests. Therefore, since it has thirty-one years of data, split sample test was applied in this watershed

for which measured streamflow data of 22 years was scaled 60% (1990-2002) for calibration to 40% (2003-2011) for validation. The value of  $R^2$  and NSE obtained during calibration were 0.89 and 0.88 respectively.  $R^2$  is used to evaluate the accuracy of the simulated value when compared with the observed values whereas; the goodness-of-fit is measured with NSE (Shimelash *et al.*, 2018). In general, the performance indices gained during the calibration and validation periods indicated an acceptable performance rate of the model in simulating the hydrological impacts of LULC changes over 1987 to 2017 periods. The graphical comparison of observed and simulated flow during validation are shown in Figure 4.10, 4.11, 4.12, 4.13, 4.14 and 4.15 for the corresponding years of study.

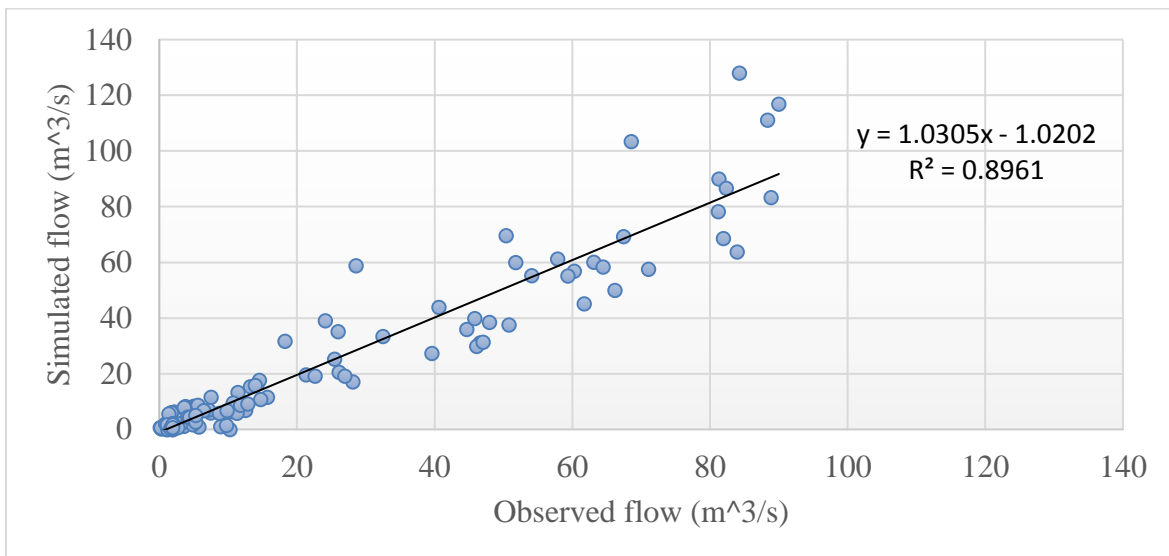


Figure 4.10 Graph of simulated versus observed flow during validation for LULC of 1987

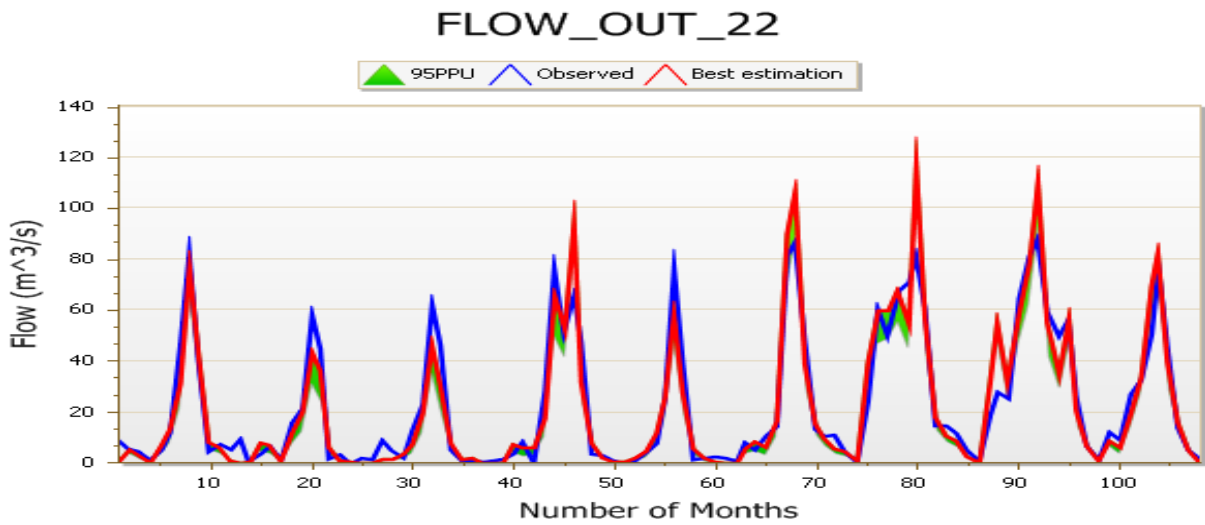


Figure 4.11 Hydrograph of Monthly simulated and observed flow during validation for LULC of 1987

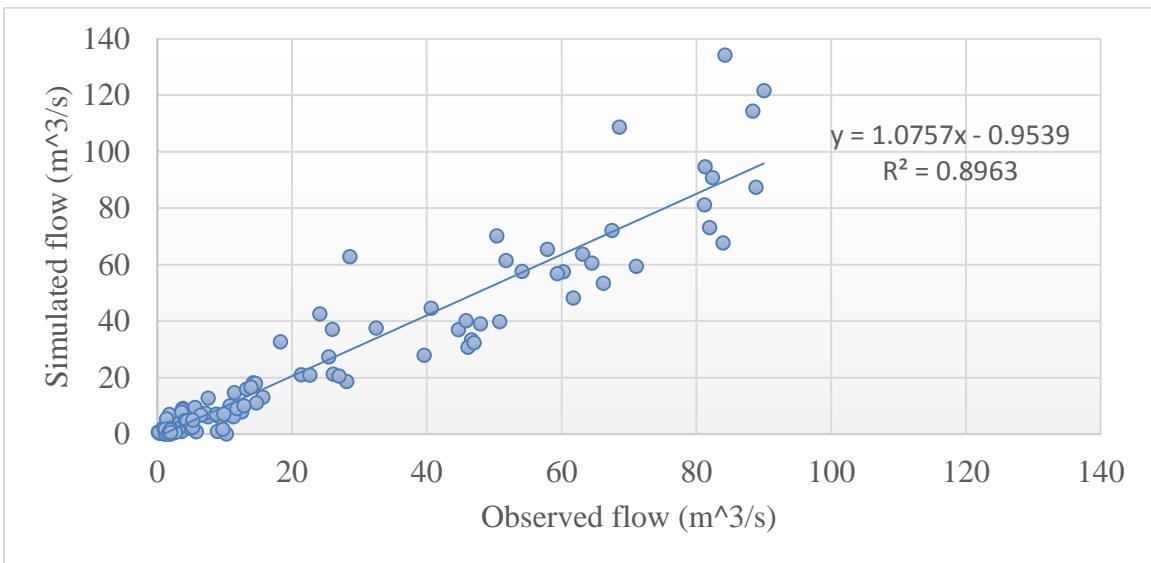


Figure 4.12 Graph of simulated versus observed flow during validation for LULC of 2001

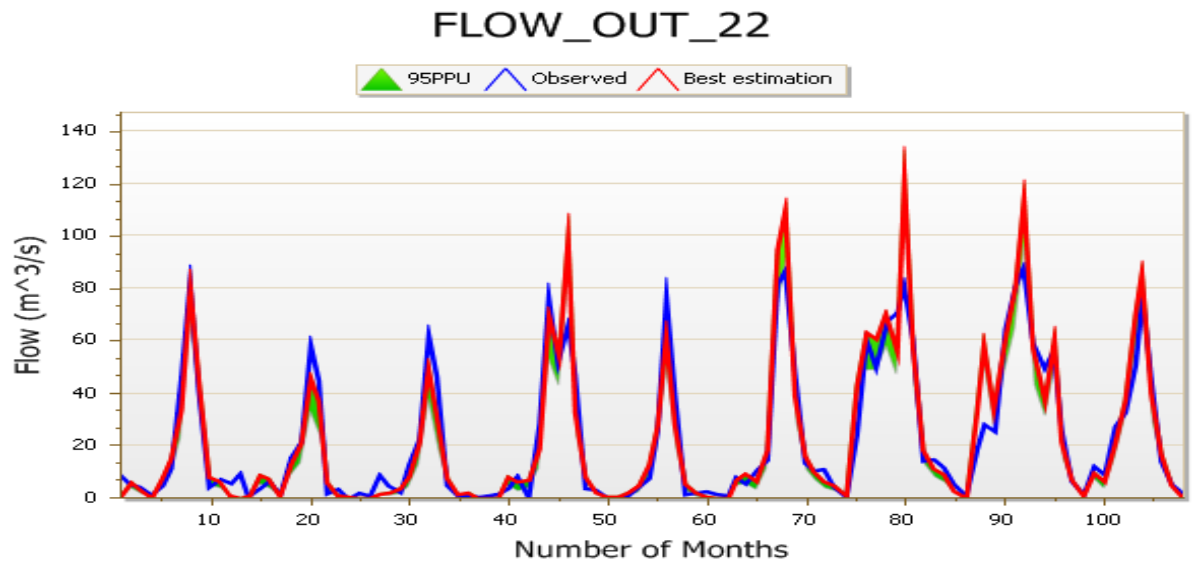


Figure 4.13 Hydrograph of Monthly simulated and observed flow during validation for LULC of 2001

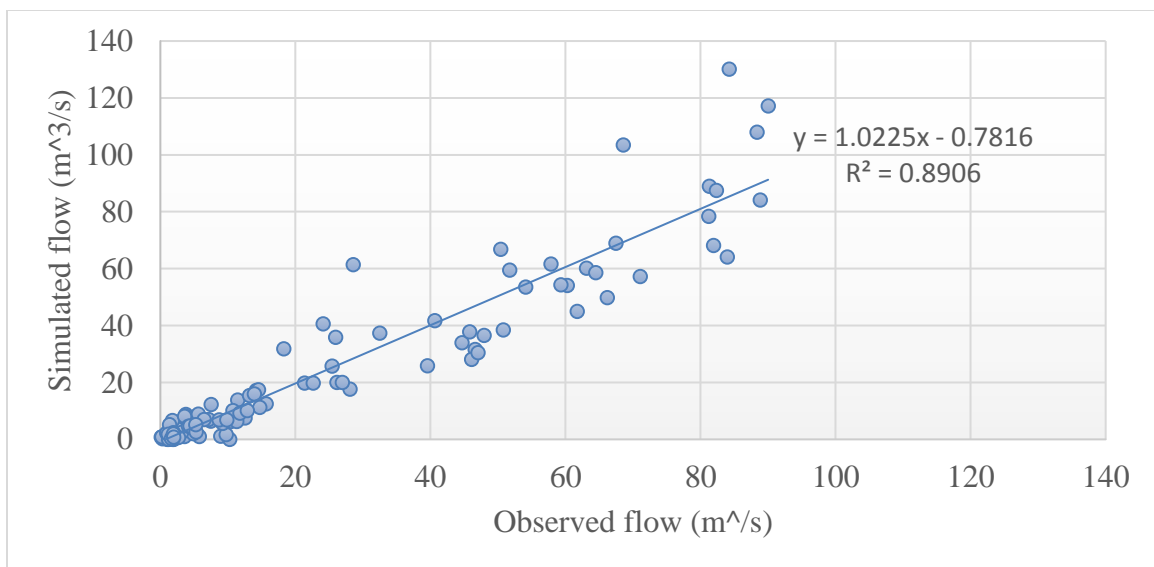


Figure 4.14 Graph of simulated versus observed flow during validation for LULC of 2017

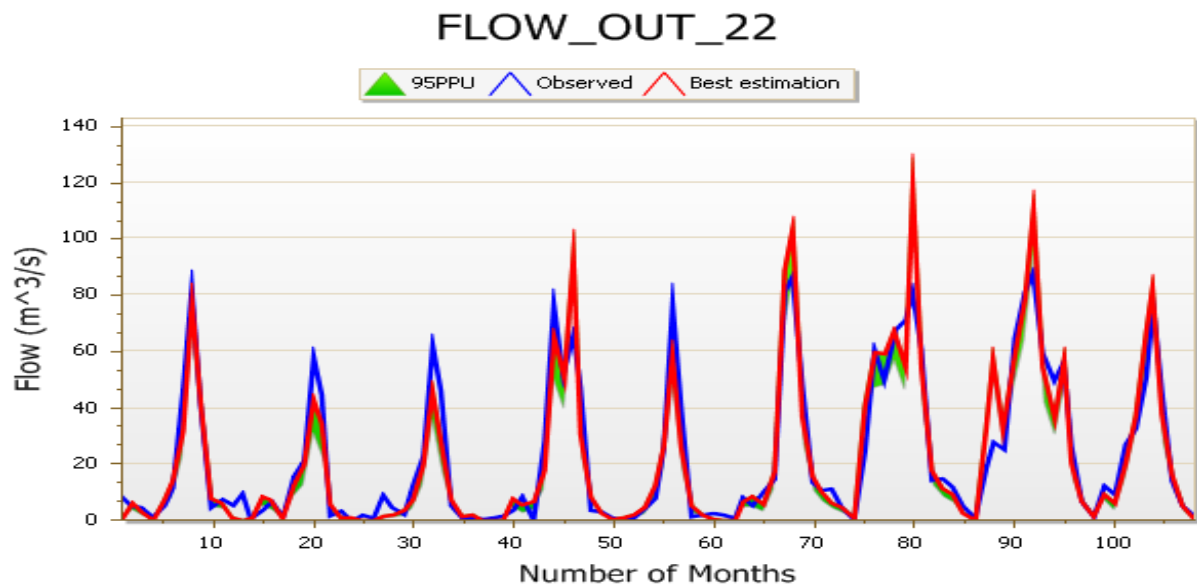


Figure 4.15 Hydrograph of Monthly simulated and observed flow during validation for LULC of 2017

#### 4.5. Model performance evaluation

Based on the performance ratings of  $R^2$ , NSE and PBIAS (Table 3.7) the SWAT model performs very good for both calibration ( $R^2 = 0.87$ , NSE = 0.82 and PBIAS = +1.4) and validation ( $R^2 = 0.89$ , NSE = 0.88 and PBIAS = +1.2).

#### 4.6. Hydrological impacts of land use/land cover changes at the study area

##### 4.6.1. The impacts of land use/land cover change on water balance components

The study indicated that (Table 4.7), average annual surface runoff of the watershed increased from 306.55mm in 1987 LULC to 316.74mm in 2001 and to 327.42mm in 2017 LULC. Total sediment load is also increased from 209.76mm to 220.75mm to 221.32mm for LULC of 1987, 2001 and 2017 respectively. Whereas, the total aquifer recharge decreased from 336.9mm in 1987 LULC to 325.34mm in 2001 and to 312.95mm in 2017 LULC. The reduction of percolation out of soil was consistent with that of deep aquifer recharge. The annual average

total water yield of the watershed decreased from 790.26mm to 777.38mm to 766.08mm for LULC of 1987, 2001 and 2017 respectively. This changes were due to the decreased in land cover and increased cultivated land and built-up area. Covered land with natural vegetation undergone reduced surface runoff and infiltration becomes high. For the case of urbanization, land could be paved to take water in and surface runoff increased. The soil in a cultivated area could be easily detached and transported to downstream than covered land with vegetation which would be resulted in increased sediment load. For this study increased surface runoff resulted in sediment load increment. Reduction of total aquifer recharge is resulted from increased surface runoff, which reduce infiltration capacity of the soil thereby, percolation of water from soil to recharge deep aquifer is decreased. The expansion of agricultural land and built-up area over other land covers results in the increase of surface runoff following rainfall events and causes alteration in soil moisture condition and groundwater storage. The water infiltrated into the ground to recharge the shallow aquifer is reduced. Therefore, the change in the components of stream flow due to LULCC is expected to decrease dry season discharge which mostly comes from baseflow (shallow aquifer contribution) and increases discharge during the wet months which supplied from surface runoff. The finding of the study is compatible with other studies carried out in different parts of the country for instance, by Mengistu (2009) in Hare Watershed, Ethiopia (the contribution of surface runoff has increased from 39% to 44% due to the LULCC occurred between the period 1975 to 2004). Similarly, the study by Gashaw *et al.* (2018) in the Andassa Watershed, Blue Nile Basin, Ethiopia indicated as surface runoff increased from 222.1mm to 233.7mm to 242.8mm in the LULC of 1985, 2000 and 2015 respectively while ground water reduced from 126.5mm to 121.9mm and 116.7 in the corresponding year respectively.

Table 4.7 The impacts of LULCC of 1987-2001, 2001-2017 and 1987-2017 periods on water balance components.

	1987	2001	2017	Rate of hanges (%)		
				1987-2001	2001-2017	1987-2017
SURQ, mm	306.55	316.74	327.42	10.19	10.68	20.87
LATQ, mm	66.96	61.28	57.79	-8.48	-5.70	-13.69
PERC, mm	336.9	325.35	312.95	-11.55	-12.40	-23.95
AQ recharge, mm	336.9	325.34	312.95	-11.56	-12.39	-23.95
ET, mm	320.5	314.4	310	-1.90	-1.40	-3.28
TSL, t/ha	209.76	220.75	231.32	4.98	4.57	9.32
TWYLD, mm	790.26	777.38	766.08	-12.88	-11.3	-24.18

Where, SURQ-Surface runoff, LATQ-Lateral soil flow, PERC-percolation, AQ-aquifer recharge, ET-Evapotranspiration, TSL –total sediment loading and TWYLD-total water yield.

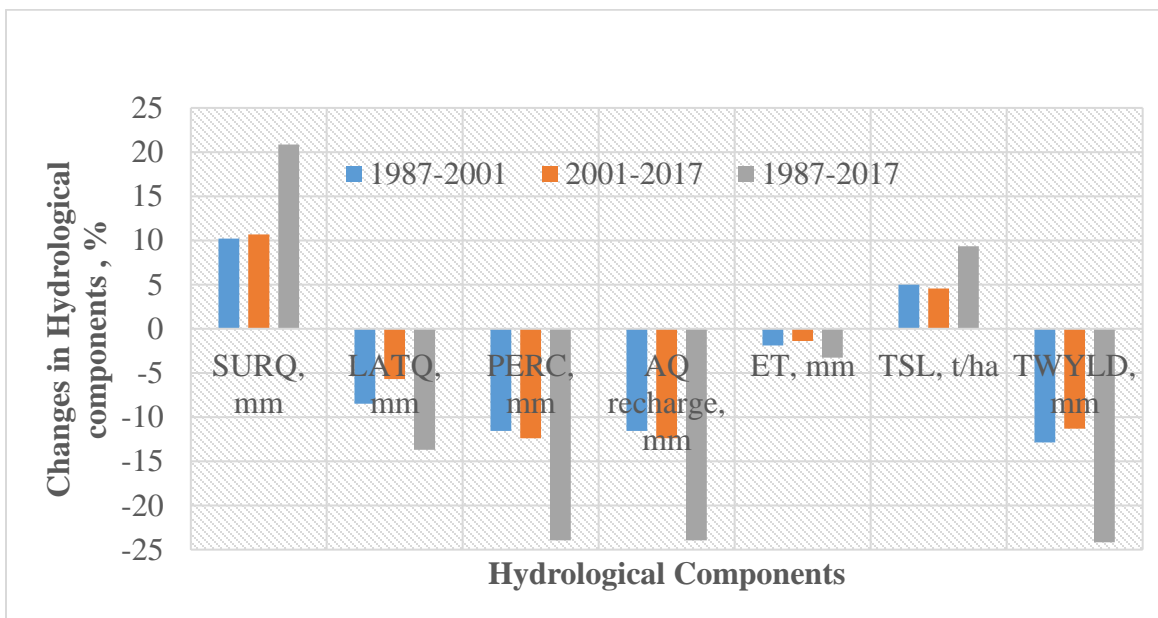


Figure 4.16 Comparison of water balance components for LULC of 1987-2001, 2001-2017 and 1987-2017

#### 4.6.2. The impacts of land use/land cover change on the streamflow

The annual stream flow through the study period is increased for wet season (June to September), and short rainy season (March to May) whereas, decreased for dry season

(October to February). The increased cultivated land and built-up area and extraction of vegetation covers (Figure 4.1) are also expected to become the reason of this change. Since land cover such as forest, grassland and range land are decreased surface runoff increased that contributed to the increment of wet and short rainy season streamflow. The infiltration rate of the watershed is reduced due to the expansion of built-up area. The reduction in infiltration rate decreased shallow aquifer from which dry season streamflow contributed. The low contributed shallow aquifer resulted in dry season streamflow reduction. The comparison of simulated stream flow for the LULC of the three periods are summarized in Table 4.8. The finding of the study is consistent with other study. For example, the result of study by Mengistu (2009) in Hare watershed indicated that mean monthly discharge for wet months had increased by 12.5% while in the dry season decreased by 30.5% during the 1992-2004 periods due to the LUCC. The study by Getachew and Melesse (2012) in the Angereb Watershed, Ethiopia has also shown that, the mean wet monthly flow for LULC of 2011 increased by 39% compared to the 1985 LULC while the dry average monthly flow decreased by 46% in 2011 compared to LULC of 1985.

Table 4.8 The impacts of LULCC of 1987-2001, 2001-2017 and 1987-2017 periods on streamflow.

Season	Annual simulated streamflow (m <sup>3</sup> /s)			Rate of changes (%)		
	1987	2001	2017	1987-2001	2001-2017	1987-2017
Wet	3930.80	4061.30	4231.20	3	4	7
Short rainy	830.90	848.70	892.70	2	5	7
Dry	1148.90	1130.90	1120.20	-2	-1	-2



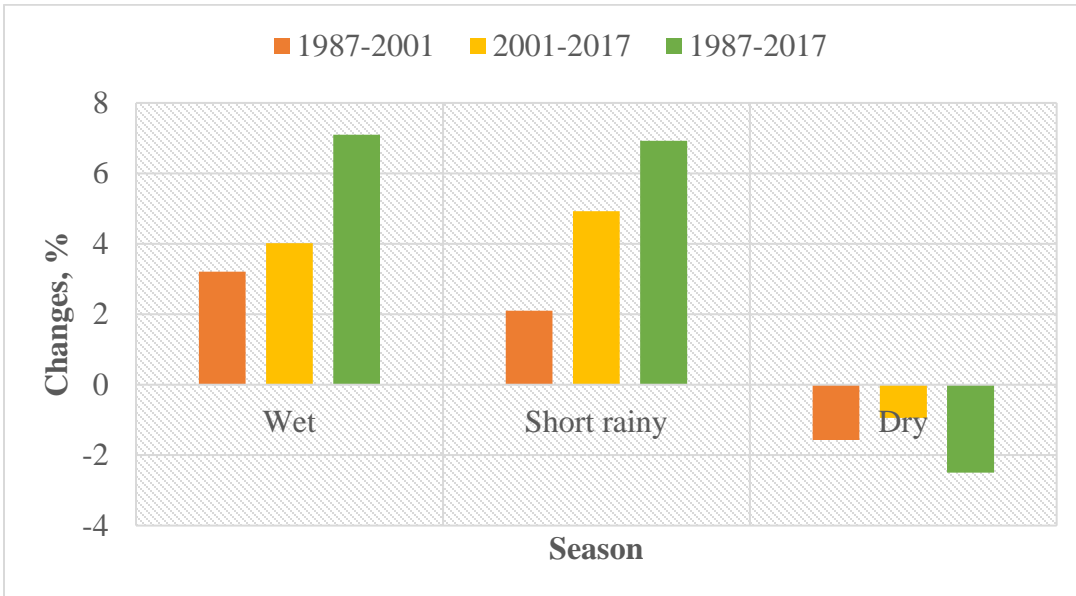


Figure 4.17 Comparison of simulated streamflow for LULCC of 1987-2001, 2001-2017 and 1987-2017 periods

## 5. CONCLUSION AND RECOMMENDATION

### 5.1. CONCLUSION

The land use and land cover change has significant impacts on the functioning of socioeconomic and environmental systems. In Ethiopia, most parts of the regions are vulnerable to problems concerning food production that mostly affects the rural livelihood mainly due to increase in population on one hand and inappropriate management of resources on the other hand. The method to investigate the impacts of land use and land cover changes on the hydrology accomplished through integrating software used to assess land use/land cover change and hydrological models used to evaluate the hydrological impacts of changes in LULC. For Hangar watershed, the assessment of LULCC by the ERDAS imagine software indicated that, forest, rangeland, grassland and water body are decreased while agricultural land and built-up area are expanded through 1987 to 2017. The SWAT model used the result of LULCCs to evaluate its impacts on the hydrology of the watershed. The SWAT-CUP used for sensitivity analysis of parameters, calibration and validation. It is found that CN2, SURLAG and CANMX are the most three top sensitive parameters in the study area. For both calibration and validation, the SWAT model performed correctly, having the value of NSE, PBIAS and coefficient of determination ( $R^2$ ) in a very good range. Generally, the study revealed that, the expansions of cultivated land and built-up area and the extraction of the forest, grassland and rangeland during the 1987 to 2017 periods had decreased the average annual total water yield contribution of the watershed (by 12.88%, 11.3% and 24.18%), lateral flow (by 8.48%, 5.7% and 13.69%), percolation from soil (by 11.55%, 12.40% and 23.95%), evapotranspiration (by 1.9%, 1.4% and 3.28%), aquifer recharge (by 11.56%, 12.39% and 23.95%) and dry season streamflow (by 2%, 1% and 2%) from 1987-2001, 2001-2017 and 1987-2017 respectively. Conversely, the LULC changes had increased surface runoff (by 10.19%, 10.68% and 20.87%), total sediment yield (by 4.98%, 4.57% and 9.32%), wet (by 3%, 4% and 7%) and short rainy season streamflow (by 2%, 5% and 7%) from 1987-2001, 2001-2017 and 1987-2017 respectively.

## 5.2. RECOMMENDATION

The significant change in the land use/land cover of the watershed area indicated from the classified LULC Map. This study revealed the hydrological process of the watershed was affected by this change. Hence, based on the result of the study, the following major recommendations are suggested:

- ❖ There should be a proper land management practices that encourage afforestation thereby, precipitation during the rainy season could be infiltrated into the ground to supply shallow aquifer (which contribute to base flow during dry months).
- ❖ Communities who are using the resources of the area should get awareness of land use/land cover change hazard to shift the trends of land use and land cover change towards increasing vegetation covers through keeping forest areas from more deforestation and covering their lands which left unproductive after erosion.
- ❖ There should be strong encouragement and support of appropriate techniques in water and soil conservation practice in the community level, so that silting-up of the surface water (which would minimizes both water quality and yield) due to the increased runoff could be reduce.

## REFERENCES

- Abbaspour, K.C., 2013. SWAT-CUP 2012: SWAT calibration and uncertainty programs—a user manual. *Eawag: Dubendorf, Switzerland*, 103.
- Abbaspour, K.C., Johnson, C.A. and Van Genuchten, M.T., 2004. Estimating uncertain flow and transport parameters using a sequential uncertainty fitting procedure. *Vadose Zone Journal*, 3(4), pp.1340-1352.
- Abraham, L.Z., Roehrig, J. and Chekol, D.A., 2007, October. Calibration and validation of SWAT hydrologic model for Meki watershed, Ethiopia. In *Conference on International Agricultural Research for Development, University of Kassel-Witzenhausen and University of Gottingen* (Vol. 5).
- Abushandi, E. and Merkel, B., 2013. Modeling rainfall-runoff relations using HEC-HMS and IHACRES for a single rain event in an arid region of Jordan. *Water Resources Management*, 27(7), pp.2391-2409.
- Allen, R.G., Pereira, L.S., Raes, D. and Smith, M., 1998. Crop evapotranspiration-Guidelines for computing crop water requirements-FAO Irrigation and drainage paper 56. *Fao, Rome*, 300(9), p.D05109.
- Arnold, J.G., Moriasi, D.N., Gassman, P.W., Abbaspour, K.C., White, M.J., Srinivasan, R., Santhi, C., Harmel, R.D., Van Griensven, A., Van Liew, M.W. and Kannan, N., 2012. SWAT: Model use, calibration, and validation. *Transactions of the ASABE*, 55(4), pp.1491-1508.
- Babar, S. and Ramesh, H., 2015. Streamflow response to land use–land cover change over the Nethravathi River Basin, India. *Journal of Hydrologic Engineering*, 20(10), p.05015002.
- Belay, S., Amsalu, A. and Abebe, E., 2014. Land Use and land cover changes in Awash National Park, Ethiopia: impact of decentralization on the use and management of resources. *Open Journal of Ecology*, 4(15), p.950.
- Beven, K. and Freer, J., 2001. Equifinality, data assimilation, and uncertainty estimation in mechanistic modelling of complex environmental systems using the GLUE methodology. *Journal of hydrology*, 249(1-4), pp.11-29.
- Beven, K.J., 2001. *Rainfall-Runoff Modeling: The Primer* Wiley. Chichester, UK.

- Bewket, W. and Sterk, G., 2005. Dynamics in land cover and its effect on streamflow in the Chemoga watershed, Blue Nile basin, Ethiopia. *Hydrological Processes: An International Journal*, 19(2), pp.445-458.
- Bewket, W., 2002. Land cover dynamics since the 1950s in Chemoga watershed, Blue Nile basin, Ethiopia. *Mountain Research and Development*, 22(3), pp.263-269.
- Blackett, M., 2014. Early analysis of Landsat-8 thermal infrared sensor imagery of volcanic activity. *Remote sensing*, 6(3), pp.2282-2295.
- Chaibou Begou, J., Jomaa, S., Benabdallah, S., Bazie, P., Afouda, A. and Rode, M., 2016. Multi-site validation of the SWAT model on the bani catchment: model performance and predictive uncertainty. *Water*, 8(5), p.178.
- Chase, T.N., Pielke Sr, R.A., Kittel, T.G.F., Nemani, R.R. and Running, S.W., 2000. Simulated impacts of historical land cover changes on global climate in northern winter. *Climate Dynamics*, 16(2-3), pp.93-105.
- Denboba, M.A., 2005. *Forest Conversion, Soil Degradation, Farmers' Perception Nexus: Implications for Sustainable Land Use in the Southwest of Ethiopia (Vol. 26)*. Cuvillier Verlag.
- Devia, G.K., Ganasri, B.P. and Dwarakish, G.S., 2015. A review of hydrological models. *Aquatic Procedia*, 4, pp.1001-1007.
- Dube, T. and Mutanga, O., 2015. Evaluating the utility of the medium-spatial resolution Landsat 8 multispectral sensor in quantifying aboveground biomass in uMgeni catchment, South Africa. *ISPRS Journal of Photogrammetry and Remote Sensing*, 101, pp.36-46.
- Dwarakish, G.S., and Ganasri, B.P., 2015. Impact of land use change on hydrological systems: A review of current modeling approaches. *Cogent Geoscience*, 1(1), p.1115691.
- Enderle, D.I. and Weih Jr, R.C., 2005. Integrating supervised and unsupervised classification methods to develop a more accurate land cover classification. *Journal of the Arkansas Academy of Science*, 59(1), pp.65-73.

- Garedew, E., Sandewall, M., Söderberg, U. and Campbell, B.M., 2009. Land-use and land-cover dynamics in the central rift valley of Ethiopia. *Environmental management*, 44(4), pp.683-694.
- Gashaw, T., Tulu, T., Argaw, M. and Worqlul, A.W., 2018. Modeling the hydrological impacts of land use/land cover changes in the Andassa watershed, Blue Nile Basin, Ethiopia. *The science of the Total Environment*, 619, pp.1394-1408.
- Gebeyehu A., *Regional Flood Frequency Analysis*, Hydraulics Laboratory, Royal Institute of Technology, Stockholm, Sweden, 1989.
- Getachew, H.E. and Melesse, A.M., 2012. The impact of land use change on the hydrology of the Angereb Watershed, Ethiopia. *International Journal of Water Sciences*, 1.
- Getahun, Y.S. and Van Lanen, H.A.J., 2015. Assessing the impacts of land use-cover change on hydrology of Melka Kuntrie subbasin in Ethiopia, using a conceptual hydrological model. *Hydrology: Current Research*, 6(3), p.1.
- Girmay, K.W., 2003. GIS-based analysis of land use/land cover, land degradation, and population changes. A Study of Boru-Metero Area of South Wallo, Amhara Region. Unpublished MSc Dissertation, Addis Ababa University, College of Social Science, Department of Geography.
- Guide, E.F., 2010. Technical documentation. ERDAS Inc.
- Gupta, H.V., Sorooshian, S. and Yapo, P.O., 1999. Status of automatic calibration for hydrologic models: Comparison with multilevel expert calibration. *Journal of Hydrologic Engineering*, 4(2), pp.135-143.
- Hamza, I.A. and Iyela, A., 2012. Land Use Pattern, Climate Change, and Its Implication for Food Security in Ethiopia: A Review. *Ethiopian Journal of Environmental Studies and Management*, 5(1), pp.26-31.
- <https://www.asf.alaska.edu/sar-data/palsar/>
- <https://www.earthexplorer.usgs.gov/>
- Irons, J.R., Dwyer, J.L. and Barsi, J.A., 2012. The next Landsat satellite: The Landsat data continuity mission. *Remote Sensing of Environment*, 122, pp.11-21.

- Kebede, W., Tefera, M., Habitamu, T. and Alemayehu, T., 2014. Impact of land cover change on water quality and stream flow in Lake Hawassa watershed of Ethiopia. *Agricultural Sciences*, 5(08), p.647.
- Klepeis, P. and Turner II, B.L., 2001. Integrated land history and global change science: the example of the Southern Yucatán Peninsular Region project. *Land Use Policy*, 18(1), pp.27-39.
- Kumar, N., Singh, S.K., Srivastava, P.K. and Narsimlu, B., 2017. SWAT Model calibration and uncertainty analysis for streamflow prediction of the Tons River Basin, India, using Sequential Uncertainty Fitting (SUFI-2) algorithm. *Modeling Earth Systems and Environment*, 3(1), p.30.
- Lambin, E.F., Geist, H.J. and Lepers, E., 2003. Dynamics of land-use and land-cover change in tropical regions. *Annual review of environment and resources*, 28(1), pp.205-241.
- Lin, Y.P., Hong, N.M., Wu, P.J., Wu, C.F. and Verburg, P.H., 2007. Impacts of land use change scenarios on hydrology and land use patterns in the Wu-Tu watershed in Northern Taiwan. *Landscape and urban planning*, 80(1-2), pp.111-126.
- Long, W. and Srihann, S., 2004, September. Land cover classification of SSC image: unsupervised and supervised classification using ERDAS Imagine. In *Geoscience and Remote Sensing Symposium, 2004. IGARSS'04. Proceedings. 2004 IEEE International (Vol. 4, pp. 2707-2712)*. IEEE.
- Mengistu, K.T., 2009. Watershed hydrological responses to changes in land use and land cover, and management practices at Hare Watershed, Ethiopia.
- Miheretu, B.A. and Yimer, A.A., 2018. Land use/land cover changes and their environmental implications in the Gelana sub-watershed of Northern Highlands of Ethiopia. *Environmental Systems Research*, 6(1), p.7.
- Mirzaei, M., Huang, Y.F., El-Shafie, A. and Shatirah, A., 2015. Application of the generalized likelihood uncertainty estimation (GLUE) approach for assessing uncertainty in hydrological models: a review. *Stochastic environmental research and risk assessment*, 29(5), pp.1265-1273.
- Moran, M.S., Bryant, R., Thome, K., Ni, W., Nouvellon, Y., Gonzalez-Dugo, M.P., Qi, J. and Clarke, T.R., 2001. A refined empirical line approach for reflectance factor retrieval

- from Landsat-5 TM and Landsat-7 ETM+. *Remote Sensing of Environment*, 78(1-2), pp.71-82.
- Moriasi, D.N., Arnold, J.G., Van Liew, M.W., Bingner, R.L., Harmel, R.D. and Veith, T.L., 2007. Model evaluation guidelines for systematic quantification of accuracy in watershed simulations. *Transactions of the ASABE*, 50(3), pp.885-900.
- Mtalo, F.W., Mkhandi, S.H., Jeremiah, J. and Nobert, J., 2012. Hydrological response of watershed systems to land use/cover change: A case of wami river basin.
- Muzathik, A.M., Nik, W.B.W., Ibrahim, M.Z., Samo, K.B., Sopian, K. and Alghoul, M.A., 2011. Daily Global Solar Radiation Estimate Based on Sunshine Hours. *International journal of mechanical and materials engineering*, 6(1), pp.75-80.
- Neitsch, S.L., Arnold, J.G., Kiniry, J.R. and Williams, J.R., 2011. *Soil and water assessment tool theoretical documentation version 2009*. Texas Water Resources Institute.
- OWWDSE, O. W. W. D. A. S. E. O. (2015) Orochan medium scale irrigation project
- Piao, S., Friedlingstein, P., Ciais, P., de Noblet-Ducoudré, N., Labat, D. and Zaehle, S., 2007. Changes in climate and land use have a larger direct impact than rising CO<sub>2</sub> on global river runoff trends. *Proceedings of the National academy of Sciences*, 104(39), pp.15242-15247.
- Rouholahnejad, E., Abbaspour, K.C., Vejdani, M., Srinivasan, R., Schulin, R. and Lehmann, A., 2012. A parallelization framework for calibration of hydrological models. *Environmental Modelling & Software*, 31, pp.28-36.
- Santhi, C., Arnold, J.G., Williams, J.R., Dugas, W.A., Srinivasan, R. and Hauck, L.M., 2001. Validation of the swat model on a large RWER basin with point and nonpoint sources 1. *JAWRA Journal of the American Water Resources Association*, 37(5), pp.1169-1188.
- Shen, C. and Phanikumar, M.S., 2010. A process-based, distributed hydrologic model based on a large-scale method for surface-subsurface coupling. *Advances in Water Resources*, 33(12), pp.1524-1541.
- Shen, Z.Y., Chen, L. and Chen, T., 2012. Analysis of parameter uncertainty in hydrological and sediment modeling using GLUE method: a case study of SWAT model applied to Three Gorges Reservoir Region, China. *Hydrology and Earth System Sciences*, 16(1), pp.121-132.



- Shimelash M., Tolera A. and Tamene A., 2018. Investigating Climate Change Impact on Stream Flow of Baro-Akobo River Basin. Case Study of Baro Catchment (Vol. 6).
- Singh, V.P., and Woolhiser, D.A., 2002. Mathematical modeling of watershed hydrology. *Journal of hydrologic engineering*, 7(4), pp.270-292.
- Solomon, A., 1994. Land use dynamics, soil conservation and potential for use in Metu area, Illubabor region, Ethiopia. *African Studies Series A*, 13.
- Solomon, A., 2005. Land Use Land Cover Change in the Headstream of Abbay Watershed, Blue Nile Basin, Ethiopia (Doctoral dissertation, Addis Ababa University).
- Tadele, K. and Förch, G., 2007. Impact of land use/cover change on streamflow: the case of Hare River Watershed, Ethiopia. In *Catchment and lake research, proceedings 2nd Lake Abaya research symposium (LARS), Arba Minch, Ethiopia*.
- Tegene, B., 2002. Land-cover/land-use changes in the derekolli catchment of the South Welo Zone of Amhara Region, Ethiopia. *Eastern Africa Social Science Research Review*, 18(1), pp.1-20.
- Tekle, K. and Hedlund, L., 2000. Land cover changes between 1958 and 1986 in Kalu District, southern Wello, Ethiopia. *Mountain research and development*, 20(1), pp.42-51.
- Tekleab, S., Mohamed, Y., Uhlenbrook, S. and Wenninger, J., 2014. Hydrologic responses to land cover change: the case of Jedeb mesoscale catchment, Abay/Upper Blue Nile basin, Ethiopia. *Hydrological Processes*, 28(20), pp.5149-5161.
- Tufa, D.F., Abbulu, Y.E.R.R.A.M.S.E.T.T.Y. and Srinivasarao, G.V.R., 2014. Watershed Hydrological Response to Changes in Land Use/Land Covers Patterns of River Basin: A Review. *International Journal of Civil, Structural, Environmental, and Infrastructure Engineering Research and Development (IJCSEIERD)*, 4, pp.157-170.
- User Manual, May 2014. SWAT Calibration and Uncertainty Programs - A User Manual.
- Van Liew, M.W. and Garbrecht, J., 2003. Hydrologic simulation of the little Washita river experimental watershed using SWAT 1. *JAWRA Journal of the American Water Resources Association*, 39(2), pp.413-426.
- Van Liew, M.W., Veith, T.L., Bosch, D.D. and Arnold, J.G., 2007. Suitability of SWAT for the conservation effects assessment project: Comparison on USDA agricultural research service watersheds. *Journal of Hydrologic Engineering*, 12(2), pp.173-189.

- Viera, A.J. and Garrett, J.M., 2005. Understanding interobserver agreement: the kappa statistic. *Fam Med*, 37(5), pp.360-363.
- Vilaysane, B., Takara, K., Luo, P., Akkharath, I. and Duan, W., 2015. Hydrological stream flow modeling for calibration and uncertainty analysis using the SWAT model in the Xedone river basin, Lao PDR. *Procedia Environmental Sciences*, 28, pp.380-390.
- Vogelmann, J.E., Helder, D., Morfitt, R., Choate, M.J., Merchant, J.W. and Bulley, H., 2001. Effects of Landsat 5 Thematic Mapper and Landsat 7 Enhanced Thematic Mapper Plus radiometric and geometric calibrations and corrections on landscape characterization. *Remote sensing of environment*, 78(1-2), pp.55-70.
- Wangpimool, W., Pongput, K., Sukvibool, C., Sombatpanit, S. and Gassman, P.W., 2013. The effect of reforestation on streamflow in Upper Nan river basin using Soil and Water Assessment Tool (SWAT) model. *International Soil and Water Conservation Research*, 1(2), pp.53-63.
- Yang, J., Reichert, P., Abbaspour, K.C., Xia, J. and Yang, H., 2008. Comparing uncertainty analysis techniques for a SWAT application to the Chaohe Basin in China. *Journal of Hydrology*, 358(1-2), pp.1-23.
- Zelege, G. and Hurni, H., 2001. Implications of land use and land cover dynamics for mountain resource degradation in the Northwestern Ethiopian highlands. *Mountain research and development*, 21(2), pp.184-191.
- Zeray, L., Roehrig, J. and Chekol, D.A., 2006, October. Climate change impact on Lake Ziway watershed water availability, Ethiopia. In *Conference on International Agricultural Research for Development*.

## APENDICES

### Appendix A: Parameters used in weather generator

Month	PCP_MM	PCPSTD	PCPSKW	PR_W1	PR_W2	PCPD	tmp_max	tmp_min	hmd	dewpt
Jan	9.52	0.971	4.3446	0.081	0.448	4.03	25.69	9.12	42.8	6.47
Feb	18.34	1.529	4.458	0.14	0.615	8.45	27.07	12.91	37	4.96
Mar	68.56	5.554	5.2316	0.204	0.78	16.2	27.04	13.61	42.5	7.18
Apr	79.27	5.387	4.6298	0.229	0.803	17.3	26.28	14.81	48.8	9.06
May	83.66	5.962	4.1596	0.14	0.822	14.9	24.47	13.38	63.8	12.05
Jun	139.01	5.648	1.3105	0.102	0.924	18.3	22.57	8.62	82	14.99
Jul	156.32	5.627	1.5666	0.158	0.926	22.7	21.42	11.45	88.4	15.42
Aug	216.07	6.038	2.5833	0.75	0.955	30.5	21.48	10.54	87.9	15.37
Sep	93.24	4.434	2.2463	0.148	0.897	19.1	22.74	12.54	84.7	15.54
Oct	75.12	4.853	4.2537	0.216	0.822	19.1	23.87	10.59	75	14.3
Nov	42.79	3.194	4.3018	0.22	0.673	13	24.41	12.52	62.6	11.74
Dec	28.99	2.739	7.052	0.12	0.694	9.71	24.89	11.1	50.3	8.46

Where;

PCP\_MM = average monthly precipitation [mm]

PCPSTD = standard deviation

PCPSKW = skew coefficient

PR\_W1 = probability of a wet day following a dry day

PR\_W2 = probability of a wet day following a wet day

PCPD = average number of days of precipitation in the month

tmp\_max = average daily maximum temperature in a month [°C]

tmp\_min = average daily minimum temperature in a month [°C]

hmd = average daily humidity in a month [%]

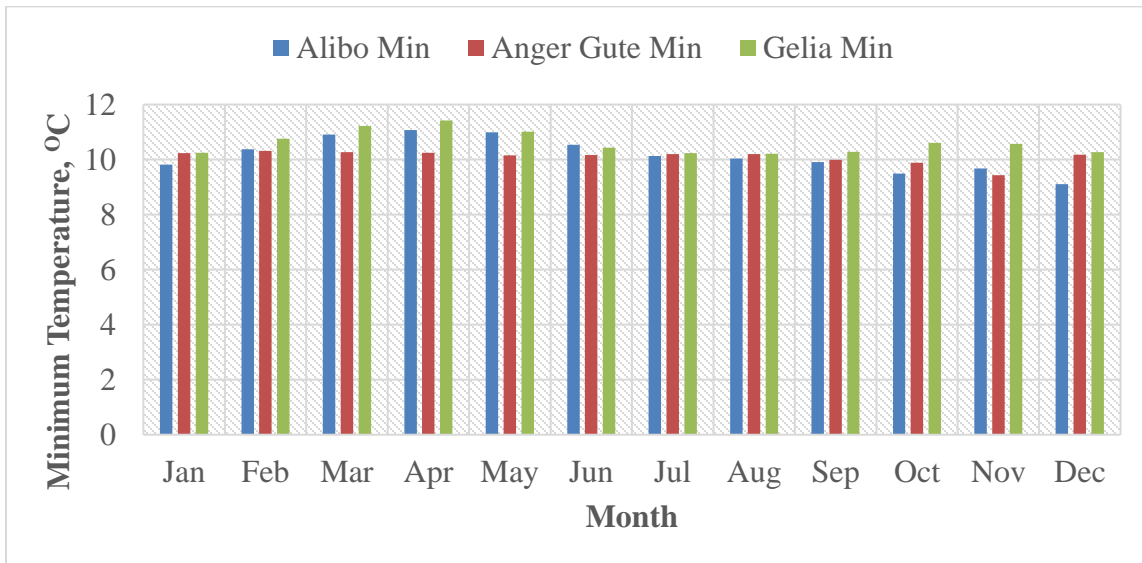
dewpt = average daily dew point temperature in a month [°C]

Appendix B: The description of sensitive parameters selected during calibration

No	Parameter Name	Descriptions
1	r__CANMX.hru	Maximum canopy storage
2	r__REVAPMN.gw	Threshold depth of water in the shallow aquifer for "revap" to occur (mm)
3	r__SOL_ALB().sol	Moist soil albedo
4	r__CN2.mgt	SCS runoff curve number
5	v__ALPHA_BF.gw	Base flow alpha factor (days)
6	v__GW_DELAY.gw	Groundwater delay (days)
7	v__GWQMN.gw	Threshold depth of water in the shallow aquifer required for return flow to occur (mm)
8	r__CH_N2.rte	Groundwater "revap" coefficient
9	r__GW_REVAP.gw	Soil evaporation compensation factor
10	r__CH_L1.sub	Base flow alpha factor for bank storage
11	r__CH_S1.sub	Available water capacity of the soil layer
12	r__ESCO.hru	Surface runoff lag time
13	r__ALPHA_BNK.rte	Plant uptake compensation factor
14	r__SLSUBBSN.hru	Manning's "n" value for the main channel
15	r__SOL_AWC().sol	Longest tributary channel length in subbasin
16	r__SURLAG.bsn	Average slope of tributary channels
17	r__EPCO.hru	Average slope length
18	r__IGRO.mgt	Land cover status code

Appendix C: Graph of average monthly minimum (a) and maximum (b) temperature of watershed

(a)



(b)

